Review

Application of Hydrogen-Bonded Organic Frameworks in Environmental Remediation: Recent Advances and Future Trends

Yu Zhang [1,†], Mengfei Tian [1,†], Zahid Majeed [2], Yuxin Xie [1], Kaili Zheng [1], Zidan Luo [1], Chunying Li [1,*] and Chunjian Zhao [1,*]

1 Key Laboratory of Forest Plant Ecology, Ministry of Education, Engineering Research Center of Forest Bio-Preparation, Ministry of Education, Heilongjiang Provincial Key Laboratory of Ecological Utilization of Forestry-Based Active Substances, College of Chemistry, Chemical Engineering and Resource Utilization, Northeast Forestry University, Harbin 150040, China; klp21zy@nefu.edu.cn (Y.Z.); 1255894206@nefu.edu.cn (M.T.); 2020223751@nefu.edu.cn (Y.X.); zkl229607@nefu.edu.cn (K.Z.); luozidan@nefu.edu.cn (Z.L.)
2 Department of Biotechnology, The University of Azad Jammu & Kashmir, Muzaffarabad 13100, Pakistan; zahid.majeed@ajku.edu.pk
* Correspondence: lcy@nefu.edu.cn (C.L.); zcj@nefu.edu.cn (C.Z.)
† These authors contributed equally to this work.

Abstract: The hydrogen-bonded organic frameworks (HOFs) are a class of porous materials with crystalline frame structures, which are self-assembled from organic structures by hydrogen bonding in non-covalent bonds π-π packing and van der Waals force interaction. HOFs are widely used in environmental remediation due to their high specific surface area, ordered pore structure, pore modifiability, and post-synthesis adjustability of various physical and chemical forms. This work summarizes some rules for constructing stable HOFs and the synthesis of HOF-based materials (synthesis of HOFs, metallized HOFs, and HOF-derived materials). In addition, the applications of HOF-based materials in the field of environmental remediation are introduced, including adsorption and separation (NH_3, CO_2/CH_4 and CO_2/N_2, C_2H_2/C_2H_e and C_eH_6, C_2H_2/CO_2, Xe/Kr, etc.), heavy metal and radioactive metal adsorption, organic dye and pesticide adsorption, energy conversion (producing H_2 and CO_2 reduced to CO), organic dye degradation and pollutant sensing (metal ion, aniline, antibiotic, explosive steam, etc.). Finally, the current challenges and further studies of HOFs (such as functional modification, molecular simulation, application extension as remediation of contaminated soil, and cost assessment) are discussed. It is hoped that this work will help develop widespread applications for HOFs in removing a variety of pollutants from the environment.

Keywords: HOFs; environmental pollutants; remediation strategies; adsorption; molecular simulation

1. Introduction

With the accelerating process of industrialization and urbanization in today's society, environmental pollution is aggravating and pollution types are becoming more and more complex, thus threatening human health and the natural environment in which we live [1]. There are many air pollutants such as particulate matter and gases and water pollution such as organic dyes, heavy metal ions, pharmaceutical and personal care products (PPCP) [2]. These pollutants involve a wide range, harmful degrees, strong aggression, and difficulty to control, even trace pollutants can cause huge environmental problems and transmit their toxicity to humans. Therefore, environmental problems have become one of the major problems urgently to be solved by human beings.

Porous materials, such as porous organic polymers (POPs) [3], covalent organic frameworks (COFs) [4], metal-organic frameworks (MOFs) [5] and hydrogen-bonded organic frameworks (HOFs) [6], have attracted more and more attention because of their broad

application prospects in the environmental remediation fields. MOFs and COFs have been extensively studied due to their high specific surface area, flexible structure, abundant porosity, and good thermal stability [7,8]. However, there are some drawbacks to MOFs and COFs. The stability of MOFs (especially in water) has always been a difficult problem to solve [9,10]. In the framework of MOFs, metal nodes have certain toxicity, which limits their application in biological and drug delivery fields. Compared with MOFs, COFs have no metal nodes, but the synthesis conditions are relatively harsh [11]. Overall, the catalysts required in the synthesis process are expensive, the reaction conditions are strict, and it is difficult to obtain large-scale crystalline products, which hinders their application and development in many fields.

Compared with traditional crystalline porous materials, HOFs have attracted extensive attention due to their unique characteristics. HOFs are pure organic framework materials that use hydrogen bonding as one of the main forces to connect the organic structure primitives with electron-acceptor bodies, and at the same time, they are formed through self-assembly in other weak interactions, such as π-π interaction, van der Waals interaction, and dipole-dipole interaction [12–16]. Actually, the history of hydrogen-bonded organic frameworks goes back even further. Figure 1a presents some crucial time points for the HOFs' development. As early as 1969, Duchamp et al. reported a two-dimensional network crystal structure formed by hydrogen bonding forces of 1,3,5-benzoic acid as an organic unit [17]. In the decades that followed, however, HOFs research stalled. In the 1990s, Wuest and his colleagues discovered a large number of HOFs, pioneering the development of diaminotriazine (DAT) groups as hydrogen bond interaction sites to construct stable hydrogen bond networks [18–21]. However, their work only focused on the crystal structure, and did not explore the pore and function of the material. Until 2011, he et al. reported the first microporous HOF material (HOF-1). Its small pore size and strong interaction with acetylene made HOF-1 can selectively separate ethylene/acetylene gas, which caused chemists to pay great attention to the development of functional materials based on HOFs [22]. Accordingly, the number of research documents related to HOFs has drastically increased every year, as shown in Figure 1b.

Because of the inherent properties of hydrogen bonds (flexibility, multi-directivity, reversibility), this means that HOFs have many advantages that differ from MOFs and COFs. First of all, compared with MOFs, HOFs are easier to synthesize and characterize and can be easily regenerated and recycled by self-healing under certain synthetic conditions [23]. In addition, HOFs have low density and low toxicity due to the absence of metal ions. Secondly, compared with COFs, the weak interaction force makes it easier for single crystals to grow, so as to obtain more detailed structural information. Most importantly, we can take advantage of the easy regulation and designability of framework structure and pore size, and design the frame structure with target structure and specific function by controlling the assembly conditions [15,24]. Furthermore, as HOFs are constructed from organic components, they generally exhibit higher chemical and thermal stability. HOFs have great potential applications in gas adsorption and separation [25,26], fluorescence recognition [27], proton conduction [28], catalysis [29], and drug transport [30] due to their large specific surface area, long-range ordered pore structure and modifiability of pore. Furthermore, HOFs have attracted vast interest in recent years because of their potential in the environmental remediation field. The major application fields of HOFs in environmental remediation are shown in Figure 2a [31–36].
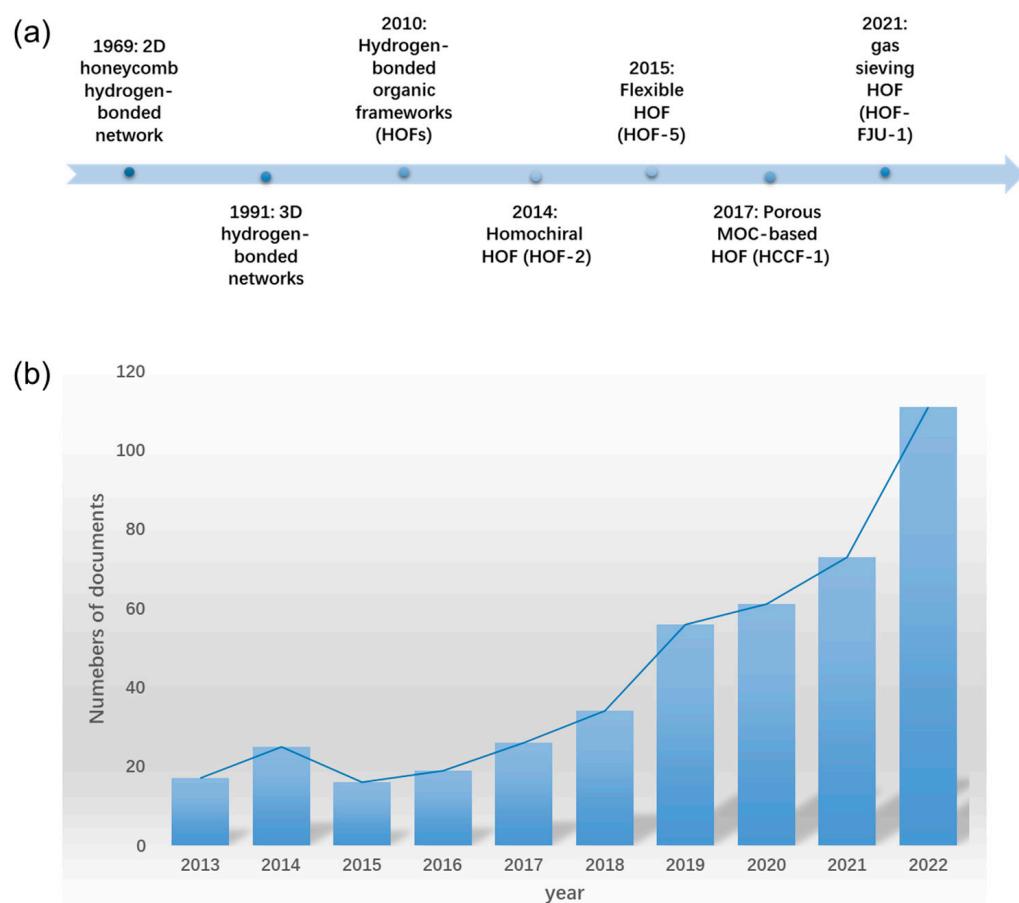
Figure 1. (**a**) Representative timeline for the development of HOFs; (**b**) Yearly numbers of documents related to HOFs, obtained from Web of Science.
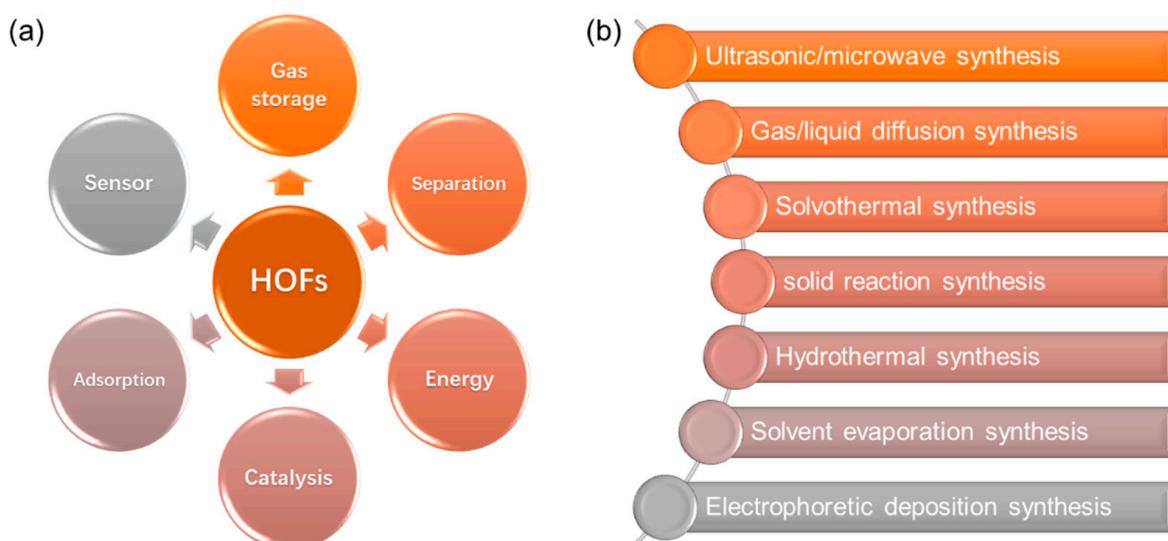
Figure 2. (**a**) Application fields of HOFs in environmental remediation; (**b**) HOFs synthesis approaches.

Metallized HOFs and HOF-derived materials can expand the application and performance of HOFs in various fields [37–39]. Based on the redox properties of metal ions and their excellent performance in light, electricity, magnetism, and catalysis, introducing metal centers into porous frameworks has become a new method to build HOFs [40]. Metallized HOFs not only strengthen the stability of building units, but also increase the adjustability

of hydrogen-bonded supramolecular frameworks, which can greatly enrich the types of HOFs [41,42]. In addition, the functional diversity of metal complexes undoubtedly provides unlimited possibilities for the creation of new multifunctional HOFs [43]. With the deepening of the research on HOFs, people begin to use HOFs to build composite materials so as to give them more abundant properties and applications. At the molecular level, by mixing HOFs with one or more additional materials and imbuing them with improved properties either physically or chemically, composites can be produced that offer the advantages of multiple materials at the same time [44,45]. In addition, HOFs-derived pyrolysis materials with high porosity can be obtained by carbonizing HOFs with dopant atoms at high temperature, which has great application prospects in energy and environment fields [37].

But in fact, developing HOFs faces many challenges. One of the reasons is that compared with the coordination bond and covalent bond in MOFs and COFs structures, the hydrogen bond force in HOFs is a flexible and weaker interaction force, which makes the pore collapse easily when HOFs remove the free solvent molecules in the pore [46]. Moreover, the weak hydrogen bonding force of HOFs cannot meet the energy requirement of the stable frame, so it is difficult to establish permanent pores. The rigidity and strength of the skeleton structure and the number of hydrogen bonding sites play a crucial role in the stability of HOFs materials. In addition, hydrogen bond interactions between structural units and guest molecules are also very important. Strong interactions between structural units and weak interactions with guest molecules are needed so that HOFs remain firm after the removal of guest molecules [47]. Figure 2b summarizes HOFs synthesis approaches [23]. The selection of different synthesis methods has different effects on the synthesis of HOFs and can create HOFs with different structures. With significant advances in the field, more and more researchers are preparing HOFs with inherent porosity, high chemical and thermal stability, and functional properties.

Due to the continuous development of the functions of HOFs-based materials and their increasing popularity in the field of environmental remediation, it is important to summarize relevant research. This work first outlines the design principles and supramolecular synthons for the construction of stable HOFs. Then, HOF modification (metallization) and HOF-derived materials (composites and HOF-derived pyrolysis materials) are summarized. Furthermore, the recent progress and application of HOFs in gas adsorption and separation, adsorption in aqueous solution, catalysis and sensing are introduced. Importantly, as a promising new environmental remediation material, we proposed selecting different functional groups to pre-design the structure of HOFs to bring additional functions, explaining the mechanism of the interaction between adsorbent and adsorbent pore sites through molecular simulation technology, and applying HOFs to the remediation of contaminated land by adsorption and chemical reduction. It is also meaningful to combine DFT high-throughput computing with machine learning to develop low-cost and efficient HOFs.

2. Design Rules of Stable HOFs

HOFs are mainly composed of monomers connected with each other through hydrogen bonding. Hydrogen bonding is a long-range force with strong non-covalent bonding and clear direction, which has a great influence on the formation of HOFs structure. Because the hydrogen bond that constitutes HOFs is much weaker than the coordination bond and covalent bond, the framework is easy to collapse and loses porosity when the solvent is lost. In addition, HOFs materials are generally crystal structures. Due to the reversibility of hydrogen bonds, the stability of HOFs materials formed is poor, which greatly limits the development and application of HOFs. In order to generate HOFs with high stability, the following methods can be adopted.

2.1. Stronger Intermolecular Interactions

In order to obtain stronger intermolecular forces from molecular assembly to HOFs formation, multiple hydrogen bond interactions between organic ligands are favorable

for the construction of stable HOFs. HOF-2 is a robust 3D porous material in which each organic building block is connected to six adjacent organic building blocks by multiple strong hydrogen bonds in 1,2-diamino-triazine groups [48]. The frame was retained after HOF-2 was soaked in different alcohols for 24 h. TGA indicates that HOF-2 is thermally stable at 350 °C. Therefore, organic molecules with multiple functional groups would be promising candidate ligands. The other approach is to create charge-assisted hydrogen bonds (especially highly charged ionic bonds) between anions and cations. For charged hydrogen bonds, the acid-base of the ligands involved is directly related to the strength of the hydrogen bond, and the combination of a strong acid and a strong base can produce permanent porosity. Nicks reported a highly stable HOF based on strong charge-assisted hydrogen bonding between carboxylic acid groups and amide groups [49]. Monolayer hydrogen-bonded organic nanosheets (HONs) were produced by ultrasonic-assisted liquid stripping. HONs exhibit remarkable stability, maintaining their extended crystallinity and monolayer structure even after three days of suspension in 80 °C water. Notably, the use of charge-assisted hydrogen bonding results in stronger materials.

2.2. Rigid Stereoscopic Framework

HOFs are constructed using rigid organic ligands with stereoscopic scaffolds. Although bonding of hydrogen bond units may be sensitive to desolvation in most porous organic solids with weak hydrogen bonds, some supramolecular scaffolds retain permanent porosity due to insufficient intermolecular stacking due to stereoscopic effects [50,51]. In 2020, Li et al. reported PFC-11 (PFC = Porous materials from FJIRSM, CAS), a new hydrogen-bonded organic framework material obtained by hydrothermal reaction using the tricarboxylic acid ligand H_3TATB as the construction unit [52]. PFC-11 can maintain a stable state for aqueous solutions and common organic solvents in the pH range of 0–10. When solvent was exchanged with ethanol and solvent molecules were removed at 90 °C, the original skeleton did not collapse. Therefore, although most organic frameworks characterized by weak hydrogen bonds are sensitive to solvent removal, there are still some rigid skeletons with inherent pores. To sum up, a rigid stereoscopic framework plays a crucial role in the stability and permanent porosity of HOFs, which is helpful to the construction of HOFs.

2.3. Highly Interpenetrated Networks

Proper introduction of interpenetrating structure into the HOFs skeleton is also an effective means to improve the stability of HOFs. It is well known that interpenetration reduces aperture but enhances skeleton stability because interpenetrating frames have lower energy and are thermodynamically advantageous. By controlling crystallization conditions (e.g., solvent, temperature), interpenetrating frames are easily achieved (e.g., polycarboxylic acids). Hu et al. used interpenetration to construct a diamond topology network of HOF-TCBP (H_4TCBP = 3,3′,5,5′-tetrakis-(4-carboxyphenyl)-1,1′-biphenyl) with permanent three-dimensional porous structure and five-fold interpenetration structure [53]. The activated HOF-TCBP has a high specific surface area of 2066 $m^2 \cdot g^{-1}$, which can adsorb and separate light hydrocarbons with high selectivity. More importantly, the structure of HOF-TCBP did not change after soaking in water and some common organic solvents for one day, and the activated HOF-TCBP could be stable to 395 °C in the N_2 atmosphere, with extremely high thermal and chemical stability, which is a rare combination of HOF structures. The interpenetrating frame constructed by modifying the structure of the building unit and adjusting the assembly conditions plays an irreplaceable role in the thermal and chemical stability of HOFs

2.4. Additional Intermolecular Interaction

Although HOFs are formed primarily through self-assembly through intermolecular hydrogen bond interactions, additional intermolecular forces can also stabilize the construction of HOFs. Weak interactions between molecules, such as π-π stacking, are

also important driving forces for stabilizing organic porous solids. The solid redox active hydrogen-bonded organic framework CPHATN-1a is formed by using the hexaazatri-naphthalene (HATN) unit [54]. The hydrogen bonds and strong π-π interactions between organic ligands form a stable HOF with the periodic arrangement. CPHATN-1a has good solvent resistance and prevents solvent hydrolysis. Therefore, the existence of π-π packing can further enhance the stability of the framework structure and obtain excellent stability of HOFs.

2.5. Avoiding D/A Structure

Avoid the presence of donors and recipients that form terminal hydrogen bonds. HOFs generally show poor stability in highly polar organic solvents such as dimethyl sulfoxide, while highly polar solvents are generally good hydrogen bond donors/acceptors and can form strong hydrogen bonds with organic ligands, resulting in leaching and etching of organic molecules from HOFs. Therefore, weakly polar solvents such as tetrahydrofuran, dimethyl ether, and isopropyl alcohol should be used in the synthesis of HOFs [52,55]. These HOFs can remove solvent molecules from the pores at room temperature during the activation process to ensure the integrity of the frame. Therefore, avoiding the formation of D/A structures is crucial for the construction of high porosity and stable HOFs.

In conclusion, the construction of stable HOFs still requires the coordination of the above strategies, namely, the combination of directional hydrogen bond construction units and rigid organic framework of co-planar p-conjugated large aromatic molecules. This enables porous HOFs with strong intermolecular interactions, which play a critical role in achieving molecular stability and permanent porosity.

3. Supramolecular Synthons for Designing HOFs

3.1. DAT Synthons

Diaminotriazines (DAT) are commonly used synthons for the construction of porous HOFs materials. The DAT functional group contains two amino and nitrogen atoms, which can be used as hydrogen bond acceptors or donors, and between the two DAT through N—H···N hydrogen bonds can form three kinds of supramolecular synthons with different structures. The remaining two amino groups of each DAT dimer are interlinked with neighboring DAT by hydrogen bonds, thus extending into a two-dimensional or three-dimensional hydrogen bond network (Figure 3a). A series of diaminotriazine HOFs can be constructed by using this property [56–58]. Wuest and colleagues prepared the first diaminotriazine HOFs [19]. Later, He et al. combined DAT into the main chain to synthesize 3D micropore HOF, HOF-1 with permanent porosity [22]. The BET of HOF-1 is 359 $m^2 \cdot g^{-1}$, and the thermal stability is up to 420 °C. It can selectively separate C_2H_2/C_2H_4 under environmental conditions. At the same time, a series of diaminotriazine HOFs with different crystal structures, pore shapes, sizes, and functions have been reported successively. Some reported synthons for the construction of diaminotriazine HOFs are shown in Figure 3b.

3.2. Carboxylic Acid Synthons

Carboxyl ligands are the simplest functional group to form hydrogen bonds. As shown in Figure 4a, there is only one type of hydrogen bonds: O—H···O [59], it not only has a strong force but also has a strong direction. The construction units are connected by carboxylic acid dimers to form a honeycomb hydrogen bond network or two-dimensional layer with two-dimensional folds. Therefore, carboxy ligands are very suitable for the construction of porous HOFs.

(a)

(b)
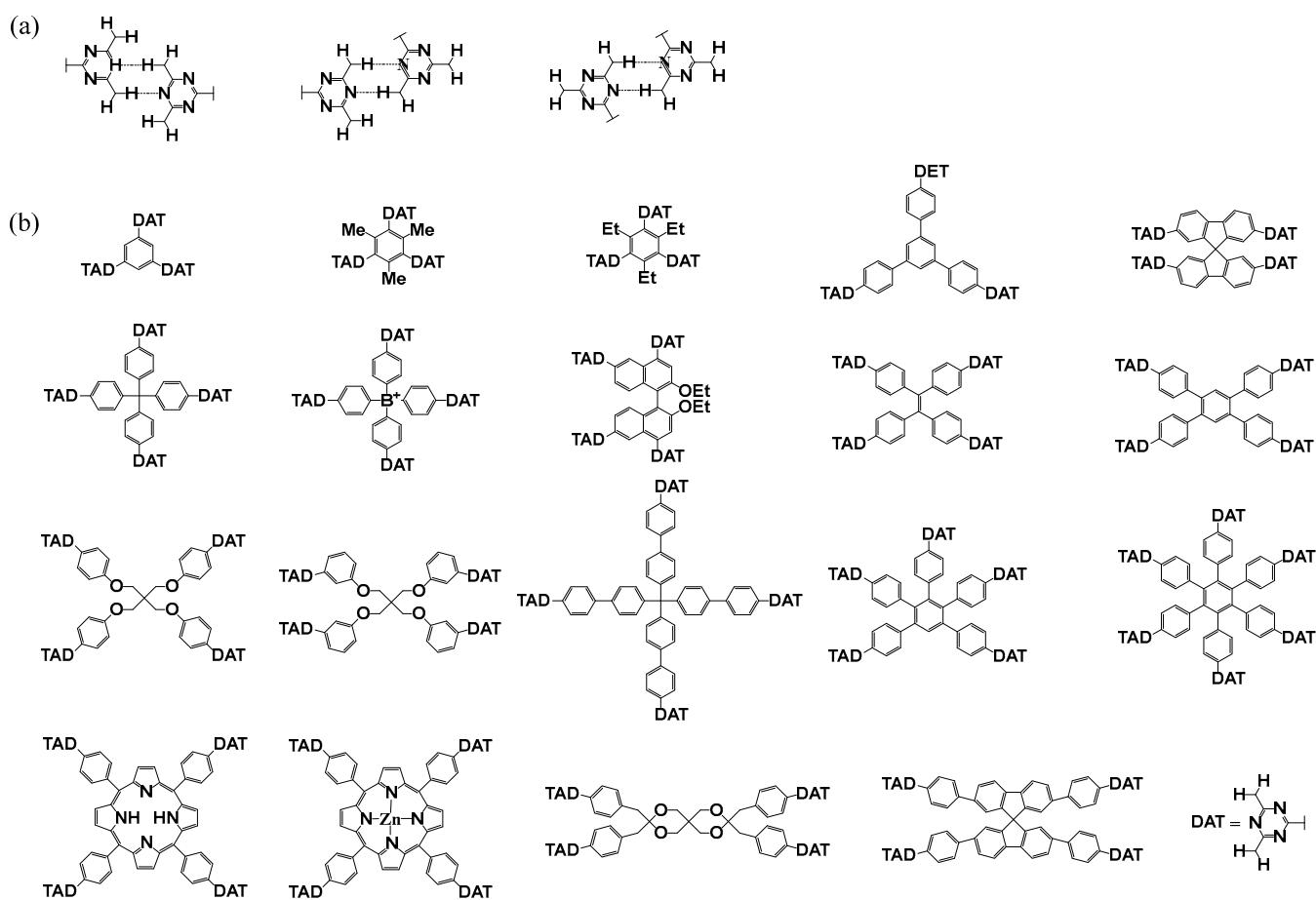
Figure 3. (**a**) Types of hydrogen bonds formed by DAT synthons; (**b**) Part of the DAT synthesis substructure has been used to construct HOFs.

(a)

(b)
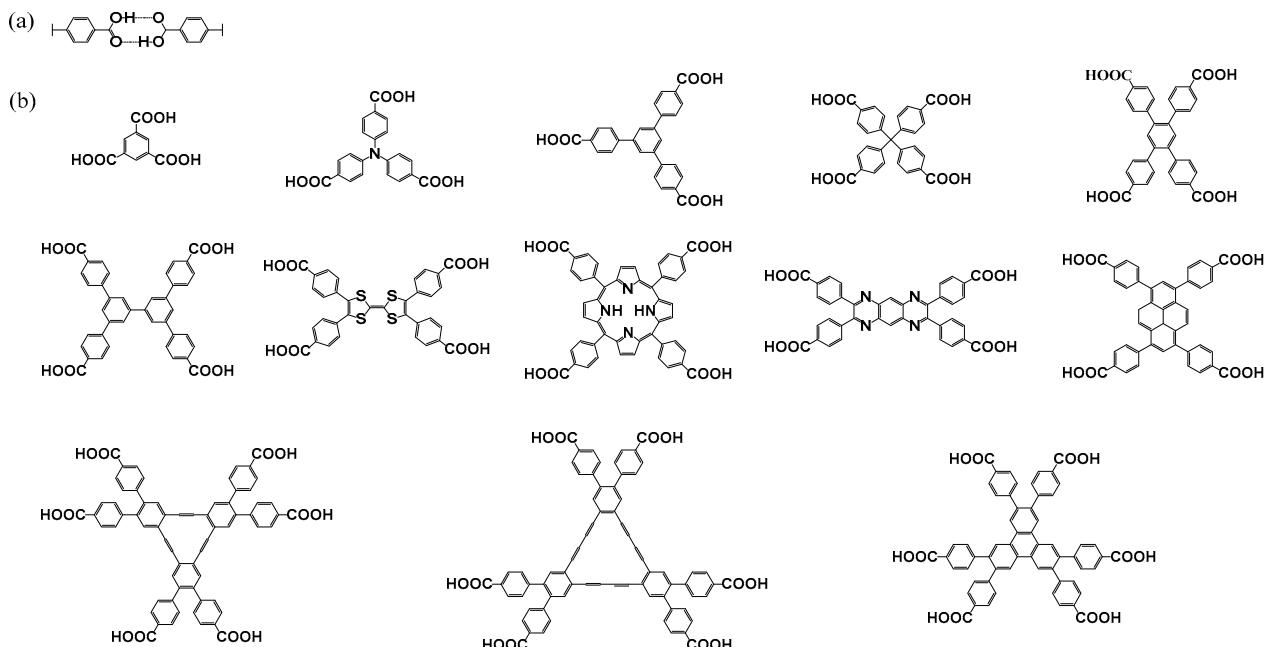
Figure 4. (**a**) The way hydrogen bonds are formed by carboxylic acid synthons; (**b**) Part of the carboxylic acid synthesis substructure has been used to construct HOFs.

Figure 4b shows the structural formula of carboxylic acid synthons selected for some carboxylic acid HOFs. The carboxylic acid synthons form simple hydrogen bonds and mature mechanisms, which are the most mature synthons in HOFs synthesis. Many recently reported carboxylic acid synthonic structures contain carboxyphenyl instead of carboxylic groups, which can be attributed to three reasons: (1) the introduction of carboxyphenyl improves the solubility of structures in solvents; (2) phenylene as a spacer to produce a void; (3) metal-catalyzed cross-coupling reactions between aryl groups have been commercialized, allowing the easy synthesis of various structures. In 2021, Yu et al. selected N,N,N′,N′-tetra-(4-carboxyphenyl)-1,4-phenylenediamine (H$_4$TPA) as synthons to assemble microporous HOFs in alcohol solutions of different polarities and named them HOF-30 [60]. The HOF-30 has a 3D decad interpenetrating network structure, with the narrowest channel size of about 3.5 Å along the direction. The solvent-removed HOFs (HOF-30a) also retained the 3D decad interpenetrating network structure, and the channel size was about 4.2 Å along the A-axis.

3.3. Pyridine Synthons

Small organic molecules containing pyridine modules have also been used in the construction of HOFs because the N atom in pyridine has a good electron-donating ability and can form strong hydrogen bonds with the H atom. As with the carboxyl group, two pyrazole functional groups are connected by N—H⋯N hydrogen bonds interconnect to form stable HOFs (Figure 5a) [23]. Some reported synthons for the construction of pyridine HOFs are shown in Figure 5b. It is worth noting that in the reported pyrazole cycle-based HOFs, the pattern of hydrogen bonds between the pyrazole cyclids at the end of the trunk is not the same as that of paired hydrogen bonds between carboxyl groups. Luo et al. synthesized a HOF (HOF-8) using tris (4-pyridyl)-1,3,5-triamidobenzene (TPBTC), which has good selectivity for benzene adsorption [32]. Moreover, the activated HOF-8 still maintains its structural integrity even at 350 °C. Even in MOFs and COFs, a material with such high thermal stability is very limited.
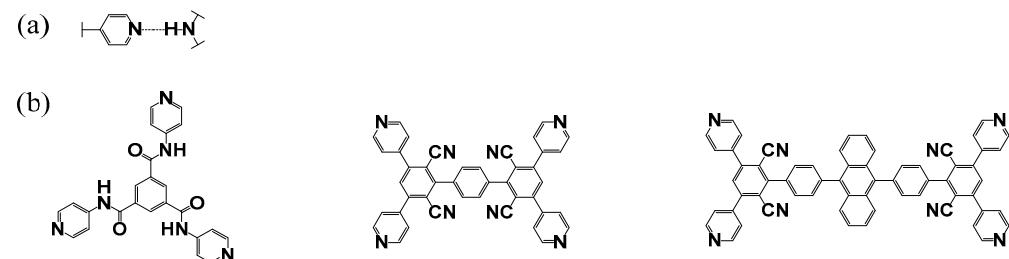

Figure 5. (**a**) The way hydrogen bonds are formed by pyridine synthons; (**b**) Part of the pyridine synthesis substructure has been used to construct HOFs.

3.4. Sulfonate-Guanidium Sheet Synthons

In the process of supramolecular self-assembly, the guanidinium cations (G = C(NH$_3$)$^{3+}$) with triple axial symmetry and organic sulfonic root ions (S = R-SO$_3^-$) can be connected by a hydrogen bond to form a honeycomb sulfonic acid-guanidinium (GS) hydrogen bond network. Sulfonate-guanidine is one of the most common two-component supramolecular synthons, and the relationship between G and S is not only through multiple N—H⋯O—S hydrogen bonds are connected to each other (Figure 6a), there is electrostatic action, and GS grid has the good folding ability, so using different organic sulfonate ions and guanidine cations self-assembly can become very rich structure [61]. The structural formulas of some sulfonic acid synthons that can form sulfonic acid HOFs are summarized in Figure 6b. In 2019, Kang et al. dissolved tetra-(4-sulfonyl)methane and guanidine hydrochloride in a mixed solvent of methanol and acetone, and then diffused slowly into the mixed solvent through methylene chloride vapor, and finally formed a sulfonic acid HOFs with ammonia adsorption properties in the solution, named Korea University Framework-1

(KUF-1) [62]. KUF-1 has a thermal stability of up to 300 °C and is completely regenerated at room temperature and vacuum.

(a)

(b)
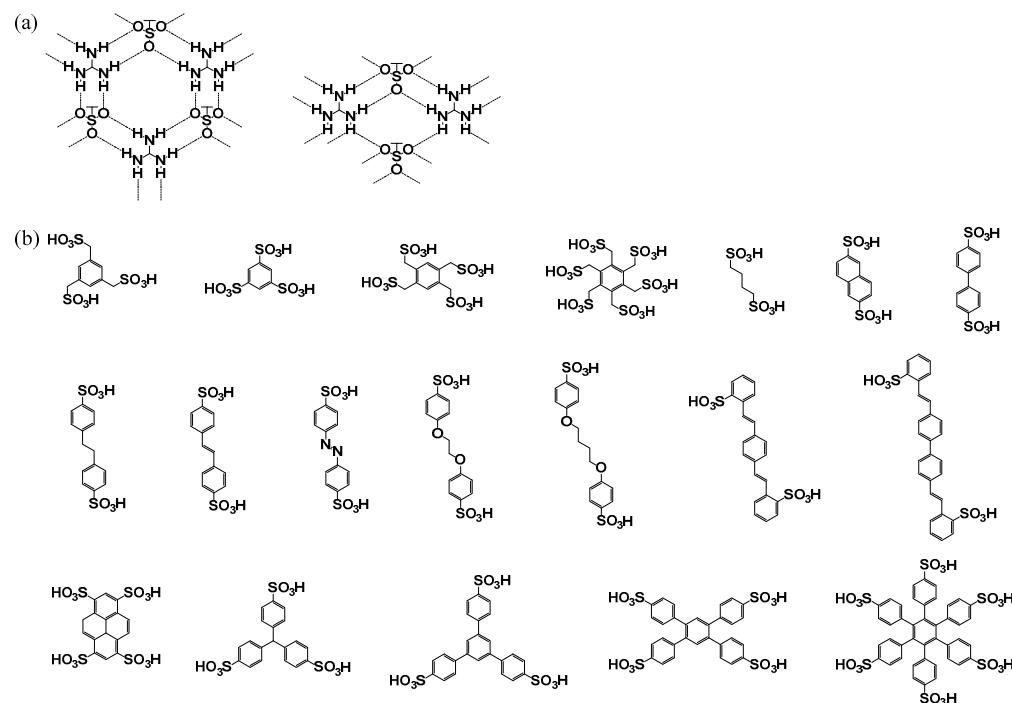
Figure 6. (**a**) Types of forming hydrogen bonds between sulfonic acid and guanidine; (**b**) Part of the sulfonate synthesis substructure has been used to construct HOFs.

3.5. Carboxyl-Pyridine Dimer Synthons

The carboxyl-pyridine dimer is also a common two-component supramolecular synthons, and the dimer has the double hydrogen bonds effect of O—H···N and O···H—C (Figure 7) [63,64]. Lü's research group reported the synthesis of a hydrogen-bonded 3D supramolecular organic framework (SOF-7) using 1,4-bis(4-(3,5-dicyano-2,6-dipyridyl) dihydropyridyl)benzene and 5,5′-bis (acetylamino)diisobenzoic acid as binary building blocks [65]. The material starts with an O—H···N hydrogen bond and has a quadruple interpenetrating structure, good thermal stability at 350 °C, excellent structural durability against water and organic solvents, and permanent porosity.
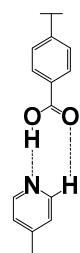
Figure 7. The way of forming hydrogen bonds between carboxyl and pyridine.

Although the structural formulas of synthons are varied, there are still some problems, such as the synthesis process being relatively complex, the hydrogen bond formation type being relatively complex, and the hydrogen bond formation mechanism being immature. These problems will affect the preparation of other synthons and the synthesis of other HOFs. The comparisons of different supramolecular synthons for designing HOFs are summarized in Table 1.

Table 1. Comparison of different supramolecular synthons for designing HOFs.

Supramolecular Synthons	Construction Component	Hydrogen Bonding Mode	Numbers of Hydrogen Bond Type	Chemical Stability
DAT	Single-component	N—H⋯N	3	Good
Carboxylic acid	Single-component	O—H⋯O	1	Good
Pyridine	Single-component	N—H⋯N	1	Good
Sulfonate-guanidium sheet	Two-component	N—H⋯O—S	2	Sulfonic acid is unstable
Carboxyl-pyridine dimer	Two-component	O—H⋯N and O⋯H—C	1	Good

4. HOFs Modification/HOF-Derived Materials

The inherent characteristics of HOFs, such as large specific surface area, long-range ordered pore structure, and modifiability of pore, provide favorable conditions for the application in environmental remediation. However, the framework of HOFs is easy to collapse and the poor solubility and dispersion in most solvents limit the catalytic activity and adsorption performance. Therefore, it is necessary to provide additional physical and chemical properties for HOFs to meet the needs of practical applications. Various HOFs modification (metallization) and HOF-derived materials (composites and HOF-derived pyrolysis materials) have received wide attention and development. The comparisons of HOFs modification are summarized in Table 2.

Table 2. Comparison of HOFs modification.

Materials		Guest Species/Other Materials	Porosity	Obtaining Property
Metallized HOFs	Metal-organic cations	$[M(H_2O)_6]^{n+}$ (n = 1, 2, 3⋯); $[M(NH_3)_6]^{n+}$; $[M(en)_3]^{n+}$; $[M(tame)_2]^{n+}$; $[M(lmdz)_6]^{n+}$; Metal-organic cage $[M(CN)_n]^{m-}$ (n = 2, 3, 4⋯; m = 1, 2, 3⋯); $[M(C_2O_4)_n]^{m-}$	Microporous	Oxidation-reduction; Electronics; Optics; Magnetism
	Metal-organic anions			
	Neutral metal-organic complexes	Metal salt hydrate		
	Metal-porphyrin complexes	Metal centers of porphyrins and their derivatives		
HOF composites		Nanoparticles; Metal oxides; Polymers; Carbon materials	Micro/mesoporous	Catalysis; Adsorption; Photothermal
HOF-derived pyrolytic materials		Heteroatoms	Micro/mesoporous	Oxidation-reduction; Adsorption

4.1. Metallized HOFs

Metal ions with different valence states (neutral, positively charged, or negatively charged) have been widely used as effective catalysts [66–68]. Based on the redox characteristic of metal ions and their excellent performance in optical, electric, magnetic, and catalytic aspects, metal centers are introduced into porous frames as a new method to construct porous materials. The modular nature of HOFs allows for integration through various molecular building blocks and for these molecular building blocks (i.e., organic ligands) to be evenly distributed throughout the HOFs. It is worth mentioning that some metallized HOFs are achieved by using metallized monomers such as metallized porphyrin monomers [69,70].

4.1.1. Metallized HOFs Containing Metal-Organic Cations

Cationic metal complexes can be combined with anionic sulfonates or phosphates because they can replace water or ammonia molecules that coordinate with metals to form structurally stable HOF mixtures [71,72]. In addition, various amines such as "en" (ethylenediamine) and "tame" (1,1,1-tri(aminomethyl)ethane), "lmdz" (imidazole), etc., are also used

in the construction of metallized HOFs containing organic cations [73–76]. Assembling metal-organic cages (MOCs) into highly ordered, functional hybrid HOFs is also a viable strategy [77]. Luo et al. reported a series of mesoporous supramolecular frameworks based on $Co_8L_6(H_2O)_6(Y)_6$], Y = ClO_4^-, BF_4^- and PF_6^-, H_2L = 1,3-bis[(5-methyl-1h-imidazole-4-yl) methylene aminomethyl] benzene and various anions, respectively [78]. Here, the Co_8 molecular cage serves as a template for the construction of a three-dimensional mesoporous framework, and the anion Y is formed by the hydrogen bonding mode of C−H···X (X = O, F and π). It was found that the series of Co-HOFs had a cavity of a certain size, and the active site was exposed in the cavity. Moreover, the introduction of hydrogen bonds makes the structural units of the series of Co-HOF very close to the structural units of diamond-like protein crystals. Therefore, it is worth studying to construct metal-organic cations with appropriate spatial configuration to overcome the dilemma that directly affects the mixed HOFs structure.

4.1.2. Metallized HOFs Containing Metal-Organic Anions

Organometallic anions containing N or O atoms are large hydrogen bond acceptors, the most typical of which are the metalcyanide anion ($[M(CN)_n]^{m-}$) and the oxalate anion ($[M(C_2O_4)_n]^{m-}$) [79,80]. The metal-cyanide anion can be assembled with the cationic N hydrogen bond donor diamidine to form a strong hydrogen bond network. Another typical hydrogen bond acceptor metal oxalate anion can be assembled with hydrogen bond donors to form hybrid HOFs. Most of these hybrid HOFs are compact solids with low porosity or 3D frames. In addition, rigid molecules can also coordinate with metal ions to form square planar metal-organic complexes [81]. They can combine with hydrogen bond donors to form layered or pore-closed structures with overlapping accumulation. Beach et al. reacted DL-α-methylbenzylammonium with cupric pyridine dicarboxylate ions to form [α-methylbenzylammonium]$_2$Cu(PDCA)$_2$(H$_2$O) (H$_2$PDCA = pyridine-2,4-dicarboxylic acid) through acid-base reaction [82]. Methyl benzylammonium ion is oriented from edge to surface due to adjacent π···π interactions between the layers, which results in the formation of a closed stacked bilayer framework. In order to achieve the functionalization of hybrid HOF, robust and high-dimensional hydrogen-bonding entities with sufficient extension in non-planar directions need to be selected to construct stable porous HOFs.

4.1.3. Metallized HOFs Containing Neutral Metal-Organic Complexes

Hybrid HOFs' self-assembly of neutral metal-organic complexes generally requires organic ligands with metal coordination sites (N, O atoms) and hydrogen bonding sites (carboxyl, amino, imidazole, pyridine, etc.). For example, although HMAC (4-imidazolarboxylic acid) and BIPYMO (4,4′-bipyridine derivative) have two sites, the low-dimensional metal structures they form result in dense stacked structures [83]. The teeming molecular building blocks of the bulk have large spatial sites, forming a compact hydrogen-bonded supramolecular imidazole salt framework (HIF) with low porosity [84]. Moreover, even though the molecules have two sites, there are not many additional functional sites when hybridizing HOFs, which has great limitations in practical application.

4.1.4. Hybrid HOFs Containing Metal-Porphyrin Complexes

Metal-attached ligands can be bound by monomers that have the function of pre-binding ligands. Porphyrins are the most widely studied macrocyclic compounds. They play an important role in nature and have special coordination, spectral and redox characteristics. Meanwhile, the four N atoms in the center of the porphyrin ring have good coordination activity and can be modified by various metal ions to form different metal porphyrin complexes, which can be used to construct functional HOFs containing specific metal porphyrins [85,86]. Yin et al. produced a series of stable metallic porphyrins HOFs with large specific surface areas (named PFC-72 and PFC-73 series) by introducing transition metals into the center of the tetrohydroxy-carboxylate porphyrins ligand [29]. This

series of HOFs can effectively catalyze the conversion of CO_2 to CO, and cobalt porphyrin HOF shows the best performance. This work extends their use in photocatalytic reduction.

4.2. HOF-Derived Materials

4.2.1. HOF Composites

Combining HOFs with one or more additional materials and giving improved properties in physical or chemical aspects, HOF composites with the advantages of multiple materials can be obtained. Various composites have been successfully prepared, such as nanoparticles/HOF composites, metal oxides/HOF composites, polymers/HOF composites, and carbon/HOF composites [38,87–89]. Nanoparticles (NPs) have been widely used in various practical applications due to their unique physical and chemical properties [90,91]. However, their high surface energy tends to cause serious aggregation, which inevitably increases their difficulties in storage, processing and further use. HOFs are excellent framework materials that can be chemically combined with NPs as guest molecules. By introducing the guest unit into HOFs, we can obtain the HOFs that have the advantages of both the subject frame and the guest unit. Song et al. successfully prepared HOF composed of discrete organic molecular cage modules with cyanogen chloride, phloroglucinol and ammonium hydroxide, and then soaked HOF in $RuCl_3$ solution to prepare Ru^{3+}@HOF [45]. The Ru precursor was reduced by $NaBH_4$, and the Ru NPs with an average diameter of 0.47 nm were encapsulated in the HOF pore. In a similar manner, materials containing Ag NPs were prepared from $AgNO_3$ solution by HOF-101 [92]. Using HOF as Membrane filler, HOF-based Mixed Matrix Membrane (MMM) was synthesized by preparing HOF and polymer mixture solution. Lin et al. prepared HOF-PyTTA (PyTTA = 4,4′,4″,4‴ -(pyrene-1,3,6,8-tetrayl) tetraaniline)/glass fiber membrane by soaking it in HOF-PyTTA solution and drying it at 50 °C [44]. Li et al. formed a uniform dispersion by dispersing HOF-30 and PolyImide (PI) in $CHCl_3$, poured the solution into a glass plate, and stripped it for vacuum drying [89]. In addition, Liu et al. prepared HOF-based core-shell composites by ligand grafting step-by-step method [88]. Shi et al. synthesized Z-scheme hydrogen-bonded organic frameworks (HOFs)/g-C_3N_4 nanosheets (CNNS) heterojunction photocatalyst by in-situ electrostatic method [38]. The detailed synthesis methods of composites and exciting examples show that HOF composites can now be prepared by combining multiple synthesis strategies with multiple functional compounds to achieve better HOFs application efficiency.

4.2.2. HOF-Derived Pyrolytic Materials

In the last decade, a large number of MOFs [93] and COFs [94] have been used as precursors to prepare carbon materials for use in the field of environmental remediation. Similar to MOFs and COFs, HOFs consist of ordered skeletons with well-organized pores and uniformly distributed heteroatoms. In addition, since HOF is a pure organic framework that does not contain any metallic elements, it is easier to obtain clean carbon materials. In this context, the availability of HOF as a precursor for the preparation of porous carbon materials is worth further investigation. Among many heteroatomic doped carbon materials, nitrogen-doped carbon materials generally have high activity and good stability, which is the most widely studied [95]. Liu et al. prepared nitrogen and iodine-doped carbon material C_{KI} through direct pyrolysis by using an abnormally heat-stable HOF-8 constructed from nitrogen-rich ligand N,N′,N″-tri(4-pyridinyl)-1,3,5-benzenetricarboxamide (TPBTC) as a precursor and pretreated with potassium iodide (KI) [96]. At high temperatures, the presence of iodine vapor during pyrolysis expands the pore of HOF-8, resulting in a carbon material with a larger surface area, wider pore size distribution, higher pyridine N content, and a higher degree of defect sites. The results of the electrocatalytic performance of C_{KI} on the oxygen reduction reaction (ORR) show that the catalytic performance of C_{KI} is comparable to that of commercial 20% Pt/C, and can even be compared with that of MOF and COF-derived carbon, such as Co nanoparticle-embedded carbon@Co_9S_8 double-shelled nanocages (Co-C@Co_9S_8 DSNCs) and highly graphitic nitrogen-doped porous

carbon electrocatalyst (GC@COF-NC), etc. [97,98]. Therefore, this work also provides new guidance for the efficient preparation of carbon-based ORR electrocatalysts. Although HOF-derived pyrolytic materials have not yet been used in adsorption, separation, and many other environmental applications, HOF-derived pyrolytic materials, such as MOF and COF-derived pyrolytic materials, show great promise in environmental remediation.

5. Applications of HOFs in Environmental Remediation

5.1. Gas Adsorption and Separation

HOFs are a kind of crystalline porous materials with adjustable pore shape and size and modified pore surface, so they are very suitable to be used as adsorbents for gas adsorption and separation. Since most HOFs are constructed from pure organic building units, that is, HOFs usually contain only elements with small atomic weights such as C, H, N, O and S, and have a high specific surface area, HOFs as gas adsorbents can usually obtain larger mass adsorption capacity. It is possible to achieve good gas adsorption and separation performance by reasonably designing HOFs with specific pore shapes and sizes or by introducing unique adsorption sites into the HOFs framework. Table 3 concludes the adsorption and gas separation functionalities of HOFs and their derivatives.

Table 3. Gas adsorption and separation functionalities of HOFs and their derivatives.

HOFs	Pore Size/Å	BET Surface Areas $(m^2 \cdot g^{-1})$	Functionality	Ref.
SOF-1a	7.4	474	CO_2/C_2H_2 adsorption	[99]
Trispyrazole-1	16.5	1159	fluorocarbon and hydrocarbon adsorption	[51]
PFC-2	19.7, 10.7	1014	C_2H_2/C_2H_4 separation	[100]
HOF-14	31.2 × 24.1	2573	hydrocarbon separation	[101]
HOF-102	34.0 × 35.58	2500	mustard gas detoxification	[102]
benzotrisimidazole-CF$_3$	3.8	131	O_2/Ar, O_2/N_2 separatio	[103]
HOF-16a	6.7	279	C_3H_6/C_3H_8 separation	[26]
IISERP-HOF1	9.4 × 9.1	1025	CO_2/N_2 separation	[104]
HOF-9a	6.9 × 8.8	286	CO_2/N_2 separation	[105]
HOF-8d	6.8 × 4.5	-	CO_2 capture	[32]
CP-PP-1a	18.1 × 30.3	114	CO_2/N_2 separation	[106]
HOF-5a	3.9 × 5.5	1101	CO_2 capture	[36]
PFC-5	5.2 × 4.0	256	hydrocarbon separation	[107]
HOF-76a	7.0	1121	C_2H_6/C_2H_4 separation	[108]
HOF-6a	~6.4, ~7.5	130	CO_2/N_2 separation	[109]
HOF-7a	3.4 × 4.7, 4.2 × 6.7	124	CO_2/N_2 separation	[110]
HOF-11a	6.2 × 6.8	687	CO_2 capture	[55]
HOF-FJU-1a	3.4 × 5.3	385	C_2H_6/C_2H_4 separation	[111]
Tcpb/HOF-BTB	18.5	1095	CO_2/CH_4,CO_2/N_2 separation	[112]
PFC-11	-	751.3	CO_2, benzene and toluene capture	[52]
PFC-12	-	653.6	CO_2, benzene and toluene capture	[52]
HOF-12a	8.6 × 10.8	320	CO_2 capture	[113]
ZJU-HOF-1	4.6	1465	C_2H_6/C_2H_4 separation	[114]
HOF-40	4.15 × 3.85	234	Xe/Kr separation	[115]
HOF-30a	~4.2	361	propyne/propylene separation	[60]
HOF-TCBP	17.8 × 26.3	2066	light hydrocarbons separation	[53]
ZJU-HOF-10	14.07 × 16.73	1169	C_2H_6/C_2H_4 separation	[116]
HOF-4a	3.8 × 8.1	312	C_2H_6/C_2H_4 separation	[117]
UPC-HOF-6	~2.8	237	H_2/N_2 separation	[118]
SOF-7a	13.5 × 14.0	900	CO_2/CH_4 separation	[65]
CPOS-5	5.3	760	CO_2 capture	[119]

5.1.1. CO_2/CH_4 and CO_2/N_2 Separation

The main component of natural gas is methane (CH_4). Because it is a green, clean, and efficient energy, it is one of the most promising energy sources in replacing fossil fuels [120]. However, in addition to methane, natural gas also contains other unwanted impurities, such as carbon dioxide (CO_2) and nitrogen (N_2) [121,122]. These impurities will reduce the calorific value of natural gas and corrode equipment and pipelines during operation, so it is very necessary to remove these impurities. On the other hand, the burning of fossil fuels and other human activities leads to the increasing concentration of greenhouse gases (mainly CO_2) in the atmosphere, resulting in global warming [123]. Therefore, it is of great significance to capture carbon dioxide from the flue gas after combustion. In 2022, Ding et al. proposed a binary solvent synthesis strategy for the construction of C_2-symmetric molecular-based hydrogen bond organic frameworks, namely BTBA-1, PTBA-1 and TCBP-1 (BTBA = 4,4′,4″,4‴-(benzene-1,2,4,5-tetrayl)tetrabenzoic acid, PTBA = 4,4′,4″,4‴-(pyrazine-2,3,5,6-tetrayl) tetrabenzoic acid, TCBP = 3,3′,5,5′-tetrakis-(4-carboxyphenyl)-1,1′-biphenyl) [25]. BTBA-1a and PTBA-1a give significant IAST selectivity for CO_2/N_2 (20:80) mixtures at 298 K and 100 kPa, up to 2051 and 2340 (Figure 8), which are significantly higher than previously reported HOFs and comparabled to zeolite, and activated carbon selectivity, due to matching channel and CO_2 sizes [124–127]. It also shows excellent separation potential of CO_2/CH_4 mixtures.
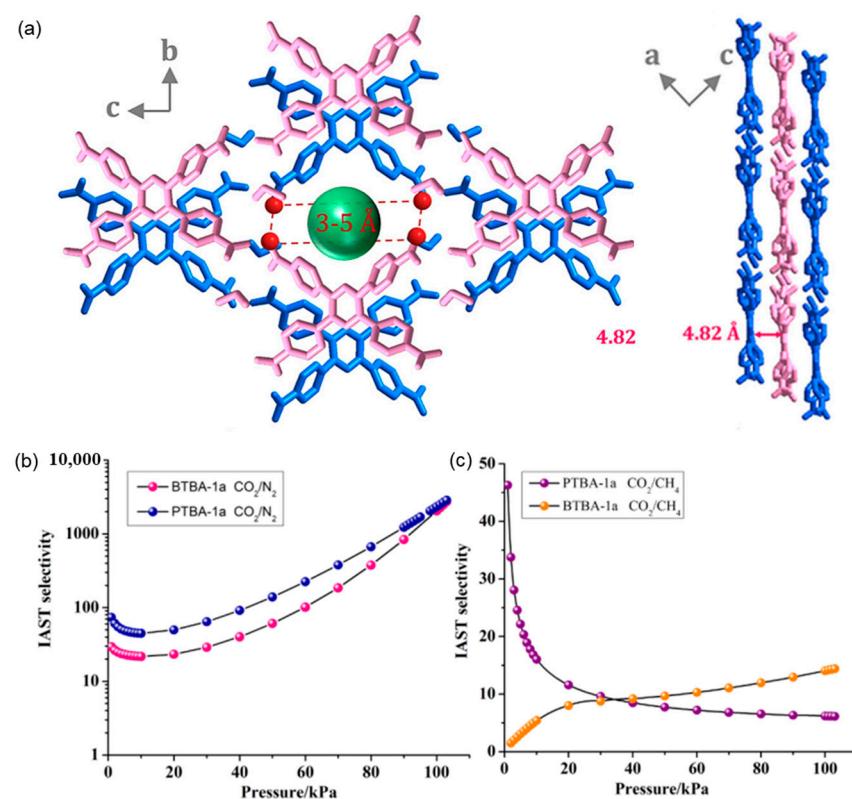

Figure 8. (**a**) Crystal structures as stick models of PTBA-1 and BTBA-1 with the same molecular stacking patterns and coplanar open oxygen atoms; (**b**) Predicted IAST selectivity of BTBA-1a and PTBA-1a for CO_2/N_2 (20:80) mixture at 298 K; (**c**) Predicted IAST selectivity of BTBA-1a and PTBA-1a for CO_2/CH_4 (50:50) mixture at 298 K. Republish from Ref. [25], Copyright (2022), with permission from Wiley.

5.1.2. C_2H_2/C_2H_4 and C_2H_4/C_2H_6 Separation

Ethylene and acetylene are important basic raw materials in the petrochemical industry. The production level of ethylene is an important index to measure the development level of a country's petrochemical industry. These low-carbon hydrocarbons are mainly derived

from naphtha cracking, and cracking gas in addition to ethylene, acetylene and byproduct ethane. In polymerization grade ethylene, the acetylene content has a very strict limit, acetylene concentration of more than 40 ppm, which will produce serious harm to the production of polyethylene, such as catalyst poisoning [128]. In addition, acetylene may neutralize metal in the pipeline and form metal acetylene compounds, which will lead to pipeline blockage and explosion. Therefore, the separation of acetylene and ethane from ethylene is of great significance [129,130]. In 2011, He's research group reported for the first time the separation of C_2H_2/C_2H_4 from HOFs (HOF-1) [22]. The molar ratio separation selectivity of HOF-1a for C_2H_2/C_2H_4 at 273K was 7.6, significantly higher than the previously reported mixed-metal-organic frameworks (M'MOFs) (<2.5) [131]. This may be attributed to the interaction between the relatively narrow pore size of HOF-1 and the H atom in C_2H_2 molecule and the amino functional group in the structure of HOF-1 material, resulting in the strong adsorption force of HOF-1 on C_2H_2. Therefore, in 2021, Zhang et al. prepared a new HOF named rod-packing desolvated framework (ZJU-HOF-1) [114]. The activated ZJU-HOF-1 has a specific surface area of 1465 $m^2 \cdot g^{-1}$ and cavity size of 4.6 Å, achieving efficient and selective separation of C_2H_4/C_2H_6. At 0.5 atmosphere and 298 K, ZJU-HOF-1 showed high C_2H_6 absorption (88 $cm^3 \cdot g^{-1}$) and C_2H_6/C_2H_4 selectivity (2.25), superior to most reported MOFs (Table 4). The breakthrough experiment on the wet C_2H_6/C_2H_4 mixture with a humidity of 60% confirmed that the presence of water vapor had no effect on the separation ability of ZJU-HOF-1, further making it an ideal adsorbent for C_2H_4 purification under real industrial conditions.

Table 4. Comparisons of C_2H_6/C_2H_4 mixture uptake and IAST selectivity between ZJU-HOF-1 and MOFs.

Absorbent	T (K)	P (Bar)	C_2H_6 Uptake$_{Mixed}$ (mmol·g^{-1})	C_2H_4 Uptake$_{Mixed}$ (mmol·g^{-1})	IAST Selectivity (C_2H_6/C_2H_4)	Ref.
ZJU-HOF-1	298	1	3.2	1.42	2.25	[114]
MFU-15	293	1	3.13	1.6	1.96	[130]
PCN-250	298	1	2.96	1.6	1.85	[132]
Ni(bcd)(ted)$_{0.5}$	298	1	2.48	1.38	1.8	[133]
IRMOF-8	298	1	2.16	1.25	1.7	[134]
MAF-49	316	1	1.21	0.44	2.7	[134]
Fe$_2$(O)$_2$(dobdc)	298	1	2.53	0.57	4.4	[135]
MIL-142-A	298	1	2.1	1.39	1.51	[136]
PCN-245	298	1	1.8	1	1.8	[137]
Cu(Qc)$_2$	298	1	1.65	0.48	3.45	[138]
ZIF-8	275	1	1.26	0.7	1.8	[139]
ZIF-7	298	1	1.2	0.8	1.5	[140]

5.1.3. C_2H_2/CO_2 Separation

Acetylene (C_2H_2) is an important fossil fuel, but also in the industry to manufacture acetaldehyde, acetic acid, benzene, synthetic rubber, synthetic fiber, and other basic raw materials. The purification of C_2H_2 from a C_2H_2/CO_2 mixture is not only valuable but also scientifically challenging due to their very similar molecular sizes and physical properties. Wang's research group reported a case of ECUT-HOF-30, a bicomponent for the separation of CO_2/C_2H_2 [141]. It is composed of $[NH_2(CH_3)_2]^+$ ion and N,N'-bis(p-benzoyl-2-yl)naphthalimide ion by self-assembly of ionic hydrogen bonds. It belongs to the microporous HOFs and has a one-dimensional rectangular channel with a pore size of 4.0 × 4.1 Å^2. The BET of ECUT-HOF-30 was calculated as 402 $m^2 \cdot g^{-1}$. It has a C_2H_2 absorption of 53.8 $cm^3 \cdot g^{-1}$ at 1 bar and 273 K, a C_2H_2 absorption of 43.7 $cm^3 \cdot g^{-1}$ at 298 K, and a CO_2 absorption of 17 $cm^3 \cdot g^{-1}$ at 273 K and 9 $cm^3 \cdot g^{-1}$ at 298 K. It has a C_2H_2/CO_2 selectivity of up to 4.8, due to the fact that C_2H_2 can form strong hydrogen bonds with carbonyl groups on the framework, and the size matches the pore size. The complete

separation of C_2H_2/CO_2 also strongly supports its superior application in the separation of C_2H_2/CO_2.

5.1.4. NH$_3$ Capture

Ammonia is a highly toxic gas, but it is also an irreplaceable chemical. It is mainly used as raw material for fertilizer, medicine, and hydrogen source [142]. So far, many porous material adsorbents have been used to capture NH$_3$ efficiently, such as MOFs, COFs, and POPs [143–147]. However, they usually exhibit a type I isotherm, that is, high selectivity but low adsorption capacity, and harsh regeneration conditions [148]. In order to overcome these deficiencies, materials with S-shaped adsorption types (types IV and V) have attracted great attention due to the presence of STEP pressure (P_{STEP}) in the isothermal curve. In 2019, kang et al. reported a case of HOFs (KUF−1) for ammonia adsorption [62]. At 298 K, its NH$_3$ isotherm exhibits an unprecedented type IV adsorption behavior, which is the first of its kind among porous materials. It is worth noting that at 298 K and 1 bar, the adsorption of NH$_3$ is 6.67 mmol·g^{-1}, about seven times that at 283 K, that is, the adsorption capacity increases with the increase of temperature, which is contrary to the adsorption trend of type I. Because it belongs to the surface adsorption at 283 K, not involved in the restructuring of the hydrogen bonds. At 298 K, hydrogen bonds participate in recombination, so the adsorption capacity is greatly increased (Figure 9). This adsorption mechanism is completely different from the open-door effect of MOFs or the mechanism of gas embedding. Of course, this particular mechanism and the characteristics of the hydrogen bonds themselves give them the characteristics of mild and lower temperature regeneration. The regeneration of KUF−1a after NH$_3$ adsorption is only required at room temperature and vacuum, which provides a new idea for the design of the NH$_3$ trapping agent.
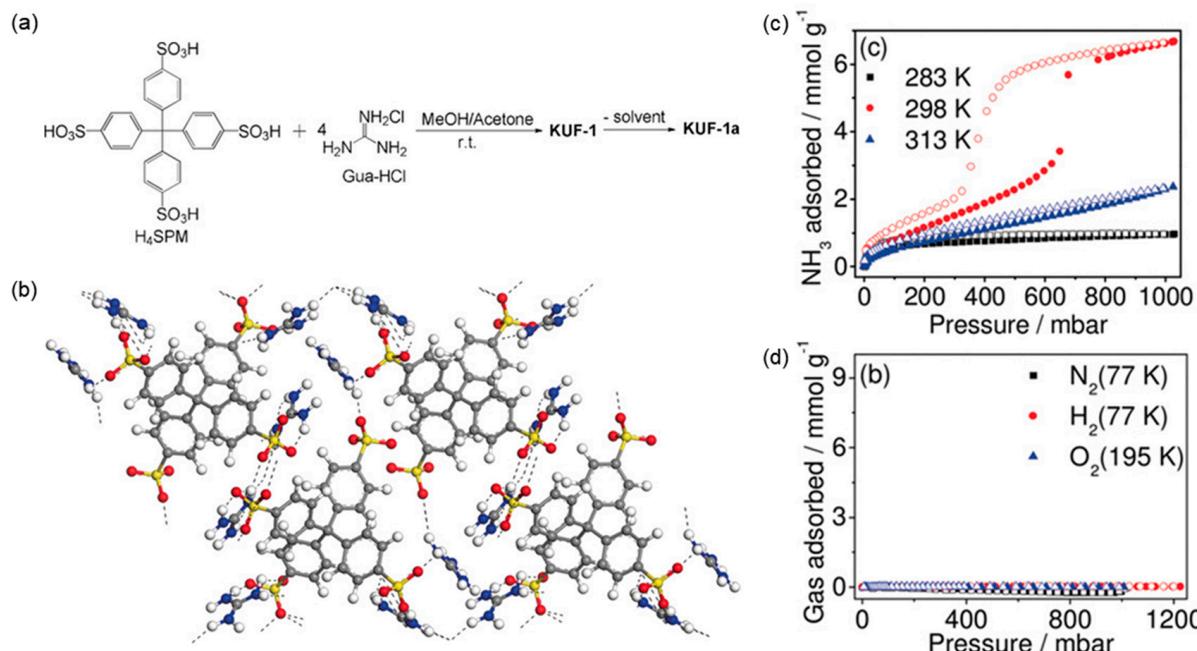

Figure 9. (**a**) Synthetic scheme of KUF−1 and KUF−1a; (**b**) Network structure showing multiple hydrogen bonds (dotted lines) among the NH groups of GuaH$^+$ and the O atoms of SPM^{4-} in KUF−1a. N blue, S yellow, O red, and C gray; (**c**) Isotherms of N$_2$, H$_2$, and O$_2$ for KUF−1a; (**d**) NH3 isotherm of KUF−1a at the indicated temperatures. Filled symbols denote adsorption and open symbols denote desorption. Republish from Ref. [62], Copyright (2019), with permission from Wiley.

5.1.5. Xe/Kr Separation

The efficient separation of xenon (Xe)/krypton (Kr) is very important for nuclear environmental detection and fuel processing. The structure and polarizability of Xe and Kr are very similar, and the traditional low-temperature distillation process consumes a lot of energy to separate Xe and Kr, so porous material adsorption separation becomes an ideal alternative separation technology. In 2019, Lee et al. synthesized highly microporous HOF (HOF-BTB) based on 1,3,5-tri(4-carboxyphenyl)benzene and first used it for Xe/Kr separation [112]. The adsorption capacity of HOF-BTB for Xe at 273 K and 295 K was 3.37 mmol·g^{-1} and 2.01 mmol·g^{-1}, respectively, while the adsorption capacity for Kr was 0.672 mmol·g^{-1} and 0.416 mmol·g^{-1}, which was much lower than Xe. Moreover, the adsorption capacity of HOF-BTB on Xe was similar to that of carbon-based porous materials, such as CC3 (2.4 mmol·g^{-1}, 295 K) and IISERP-POF8 (1.72 mmol·g^{-1}, 298 K) and MOFs without open-metal sites, such as $Co_3(HCCO)_6$ (2 mmol·g^{-1}), IRMOF-1 (2 mmol·g^{-1}) and CROFOUR-1-Ni (1.8 mmol·g^{-1}) [149–154]. The pore structure is known to be one of the key factors for Xe/Kr selectivity. The lower the largest cavity diameter (LCD)/pore limiting diameter (PLD) ratio (between 1 and 2), the higher the Xe selectivity, and the calculated LCD/PLD ratio of HOF-BTB (1.65) falls within this range. Due to its solvent stability, this recirculable water adsorption property of HOF-BTB plays an important role in industrial applications.

5.2. Adsorption in Aqueous Solution

The regular porous structure and large specific surface area of HOFs make them very suitable for the interception of macromolecules in solution. In recent years, HOFs adsorbents have made great progress and have been applied to the removal of pollutants from aqueous solutions. The adsorption of HOFs in metal ions and organic pollutants will be mainly introduced below.

5.2.1. Metal Ion Adsorption

Metal ions are difficult to biodegrade. Instead, they accumulate in organisms through the food chain and finally enter the human body. Metal ions can not only inactivate proteins in the body, but can also accumulate chronic diseases in the body. Therefore, it has always been a hot topic to alleviate metal ion pollution and protect water resources [155]. It is reported that HOFs exhibit superior adsorption performance and good adsorption effect on metal ions in water. This is because HOFs can promote the selective adsorption of natural groups and metal ions. Moreover, the abundant ordered pores of HOFs can provide active sites for the adsorption of metal ions and accelerate mass transfer. In 2022, Kaushik et al. reported a single-component HOF (^{CSMCRI}HOF-1), which is constructed with a bis(phenoxy-imine)-based organic module (PMAP, (2-((E)-(6-((E)-(2-hydroxyphenylimino)methyl)pyridin-2-yl)methylene-amino)phenol)), to extract uranium (U) efficiently [156]. The design of porous ^{CSMCRI}HOF-1 conjugated by pyridine and phenoximine provides a suitable binding site for U. In addition, ^{CSMCRI}HOF-1 has excellent stability in water, acid, alkali, salt, and high ionic strength media, and still have excellent thermal stability at 340 °C, so it is strong and durable. The synthesized HOF has a 2D porous hydrogen bond supramolecular structure, a flow channel with a pore size of 3.6~3.8 Å, and a BET surface area of 328 m^2·g^{-1}. The researchers also demonstrated for the first time that porous ^{CSMCRI}HOF-1 can be treated with the solution into large-area crystalline self-supporting films with the adjustable thickness (TFCH). The 40 nm TFCH shows excellent adsorption performance (17.80 mg U/g TFCH), which is higher than all existing adsorbents reported on uranium extraction from seawater (UES) to date (Table 5). Moreover, it has the advantages of a U/V selectivity ratio greater than 1.2 times, and long service life of five sorption-desorption cycles. This work highly reveals the great potential of HOFs in the field of metal adsorption.

Table 5. Comparison of the maximum U-adsorption capacity between [CSMCRI]HOF-1 with other materials.

Materials	Adsorbent	pH	Q_m (mg·g^{-1})	Ref.
HOFs	[CSMCRI]HOF-1	7	1185	[156]
	Cu-BTC	3	617	[157]
	MIL-101-His	6	345	[158]
MOFs	UIO-66-AO	5.5	106	[159]
	ZIF-67	4	397.6	[160]
	ZIF-90-OM	5	482.5	[161]
	COF-PDAN-AO	4	256	[162]
	COF-TpPa-1	6	120	[163]
COFs	DP-COF	4.5	317	[164]
	ACOF	4.5	169	[165]
	TPB-BPTA-COF-AO	7	90.6	[166]
	CMLH	6	99	[167]
Inorganic	Fe_3O_4@SiO_2 composites	6	52.36	[168]
	PFG MSs	8	207.6	[169]
	PAMAMG$_3$-SDB	6	99.05	[170]
Organic	CTPP	5	140	[171]
	HCP-2	8	33.4	[172]
	Ca-pretreated cystoseira indica alga	4	318.15	[173]
Biology	Bacillus cereus 12-2	5	94.14	[174]
	Biosynthesized melanin	5	49	[175]

5.2.2. Adsorption of Organic Contaminants

In environmental wastewater, we mainly focus on persistent organic pollutants (POPs). POPs refer to artificial and natural organic pollutants that can persist in the natural environment for a long time and migrate through various environmental media to produce adverse effects on the ecological environment and human health [176]. POPs are generally persistent, bioenriched, long-distance migration, and ecotoxic. POPs have strong chemical stability and cannot be decomposed by organisms. Once inside the human body, pops will accumulate in organs and cause damage. This can cause significant damage to aquatic organisms, including weight loss, fecundity failure, and developmental and immune system disorders [177,178]. The high surface area and controllable pore structure of HOFs make them very suitable for the removal of various pollutants from the environment as a new solid adsorbent. Such materials can give higher adsorption capacity to pollutants by introducing high-affinity active sites. In terms of the adsorption mechanism, the adsorption process mainly depends on hydrogen bonding, electrostatic interaction, π-π interaction, and Lewis acid-base interaction [179,180].

It has been widely reported that organic dyes are adsorbed by HOF-based materials. In 2020, Yang et al. reported the formation of 1,3,6,8-tetri (p-benzoate) pyrene through O—H···O PFC-1 assembled by hydrogen bonds and π-π interactions [181]. The synthesized HOF has a 2D porous hydrogen bond supramolecular structure, with a large channel size of 18×23 Å^2 and a surface area of more than 2000 m^2·g^{-1}. Clearly, the aperture of PFC-1 is large enough to accommodate rhodamine B (RhB) and methyl orange (MO) molecules. PFC-1 showed excellent removal capacity of RhB and MO, and the maximum adsorption capacity of 317 mg·g^{-1} and 252 mg·g^{-1} at 298.15 K, which was better than some commercially available activated carbons (58~87 mg·g^{-1} for RhB and 79.7 mg·g^{-1} for MO) [182,183]. In addition, the adsorption capacity of PFC-1 is comparable to that of some representative MOFs and COFs (Table 6). The electrostatic attraction, hydrogen bond, and π-π interaction are the main reasons for the adsorption of RhB on PFC-1, and the van der Waals force contributes greatly to the adsorption of MO. In addition, PFC-1 showed high stability and structural integrity during adsorption. In conclusion, HOFs have great potential as efficient green adsorbents for organic dyes.

Table 6. Comparison of RhB and MO adsorption capacity between PFC-1 with MOFs and COFs.

Materials	Absorbent	Dye	Q_m (mg·g^{-1})	Ref.
HOFs	PFC-1	RhB	317	[181]
	PFC-1	MO	252	[181]
	NMIL-100(Fe)	RhB	76.69	[184]
	Ni@MOF-74(Ni)	RhB	177.8	[185]
MOFs	UiO-66-NH2	MO	148.4	[186]
	ZIF-67	MO	16.3	[187]
	MIL-68(Al)/GO	MO	400	[188]
	TFP-PPDA	RhB	704.3	[189]
	CX4-BD-2	RhB	40	[190]
COFs	CuP-DMNDA-COF/Fe	RhB	378	[191]
	Benzodiimidazole-COF	MO	256	[192]
	P-TH COF	MO	25.9	[193]

In recent studies, pesticides have also been successfully adsorbed using HOFs. Lv et al. synthesized negatively charged MP-HOF using 1,3,6,8-tetra (p-benzoic acid) pyrene (H$_4$TBAPy) as the ligand [179]. The obtained MP HOF has richer oxygen-containing groups (carboxyl), π-π conjugated structure, large specific surface area, and high stability, which is conducive to their adsorption and desorption/ionization efficiency for paraquat (PQ) and chlormequat (CQ). In addition, the possible ionization mechanism was discussed, and the proposed method was successfully applied to the detection of PQ and CQ in tap water, river water, and soil, confirming its potential for practical application.

5.3. Catalysis

HOF-based photocatalytic and electrocatalytic materials are considered to be among the best candidates in the field of catalysis in terms of performance, preparation, and application, driving clean energy conversion (e.g., H$_2$ production and CO$_2$ reduction) and pollutant degradation applications [194]. HOFs based on hydrogen bond assembly often lack catalytic active centers, so it is necessary to use catalytic molecules as catalytic centers to complete the catalytic reaction. In the case of metallized HOFs, due to some special properties of metal ions (such as oxidation-reduction, and luminescence), metal complexes show excellent performance in catalysis, light, electricity, and other aspects [40]. In addition, π-π stacking, C···H···π interaction interactions, and van der Waals forces can further enhance the stability of the skeleton structure. Therefore, HOFs catalysts can be coupled with other semiconductor supporting materials, such as graphite carbonitrides and metal oxides, to form heterostructural composites [38,87]. This can complement the strengths of both and overcome their weaknesses. In addition, the carbonization of HOFs by pyrolysis is also considered a potential catalyst. Table 7 concludes the catalytic performance of HOFs-based materials.

Table 7. Summary of HOFs-based materials catalytic performance.

Materials	Reaction	Performance	Ref.
PFC-42	H$_2$O Photocatalysis	H$_2$ production rate (2265 μmol·g^{-1}·h^{-1})	[195]
TBAP-α	H$_2$O Photocatalysis	H$_2$ production rate (3108 mmol·g^{-1}·h^{-1})	[196]
PFC-72-Co	CO$_2$ Photocatalysis	CO production rate (14.7 μmol·g^{-1}·h^{-1})	[29]
PFC-73-Ni	CO$_2$ Photocatalysis	CO production rate (9.8 μmol·g^{-1}·h^{-1})	[29]

Table 7. *Cont.*

Materials	Reaction	Performance	Ref.
PFC-73-Cu	CO_2 Photocatalysis	CO production rate $(4.4\ \mu mol \cdot g^{-1} \cdot h^{-1})$	[29]
PFC-58	CO_2 Photocatalysis	CO production rate $(3.2\ \mu mol \cdot g^{-1} \cdot h^{-1})$	[86]
PFC-58-61	CO_2 Photocatalysis	CO production rate $(4.6\ \mu mol \cdot g^{-1} \cdot h^{-1})$	[86]
PFC-58-30	CO_2 Photocatalysis	CO production rate $(7.3\ \mu mol \cdot g^{-1} \cdot h^{-1})$	[86]
HOF-25-Re	CO_2 Photocatalysis	CO production rate $(1448\ \mu mol \cdot g^{-1} \cdot h^{-1})$	[197]
Pt@nano-HOF	H_2O Photocatalysis	H_2 production rate $(1480\ \mu mol \cdot g^{-1} \cdot h^{-1})$	[31]
PFC-1/CNNS	H_2O Photocatalysis	H_2 production rate $(4450\ \mu mol \cdot g^{-1} \cdot h^{-1})$	[38]
PFC-45/Cu_2O@CP	CO_2 Photocatalysis	CO production rate $(11.81\ \mu mol \cdot g^{-1} \cdot h^{-1})$	[87]

5.3.1. Energy Conversion

H_2 production and CO_2 reduction catalyzed by HOF-based materials is an important environmental catalytic application of HOFs [31,197]. Recently, it has been reported that HOF-based materials can be used as photocatalytic and electrocatalytic catalysts for water decomposition production of H_2 and CO_2 reduction to CO. In the design of HOFs, the use of π-electron-rich elements such as porphyrins can lead to semiconductor materials with excellent performance in photon absorption and electron transport. With the urgent demand for global energy and climate change, the conversion of CO_2 into high-value-added products and the reduction of CO have been a wide concern. In a study, porphyrin materials containing different metals (named PFC-72-Co and PFC-73-Ni/Cu/Zn) were constructed by simply introducing transition metals into the porphyrin structure, showing good photocatalytic activity for CO_2 reduction [29]. Remarkably, although the introduction of porphyrin core metal did not change the topological structure of the material, it caused significant changes in the non-covalent interaction between the adjacent porphyrin rings in the middle layer of the structure, orbital overlap area/area, and molecular structure. Thus, the thermal and chemical stability of the material is significantly improved (the structural integrity of metalloporphyrin HOFs can be maintained after heating at 27 °C or soaking in concentrated hydrochloric acid/boiling water for 1 day). In addition to robustness, the metallization of porphyrin centers gives the framework for different catalytic activities for CO_2 photoreduction. PFC-72-Co showed the best performance $(14.7\ \mu mol \cdot g^{-1} \cdot h^{-1})$, 1.5 times higher than PFC-73-Ni $(9.8\ \mu mol \cdot g^{-1} \cdot h^{-1})$, and 3 times higher than PFC-73-Cu $(4.4\ \mu mol \cdot g^{-1} \cdot h^{-1})$ (Figure 10). These works enrich the library of stable functional HOFs and expand their applications in photocatalytic CO_2 reduction.

Hydrogen, as a sustainable renewable energy source, is widely regarded as the best alternative to fossil fuels. In recent years, more and more attention has been paid to hydrogen production from water cracking using HOFs as catalysts. In 2020, Aitchison's research group applied the HOF material TBAP-α to photocatalytic hydrogen production [196]. The pore size of TBAP-α is 1.8×2.3 nm and has good stability. TBAP-α has excellent visible light response due to the presence of pyrene units. When the amount of catalyst TBAP-α was 1 mg·mL^{-1}, Pt and 0.1 mol·mL^{-1} ascorbic acid were used as co-catalyst and sacrificant reagent, respectively. Under visible light irradiation for 5 h, the hydrogen generation rate reached 3108 μmol·g^{-1}·h^{-1}, which was 20 times that of amorphous 1,3,6,8-tetrapyrene (4′-carboxyphenyl) (TBAP) under the same conditions. Using monochromatic light from LED sources, TBAP-α has an external quantum efficiency (EQE) of about 4.1 % at 420 nm, this is higher than many conjugated polymer catalysts such as 4,8-di(thiophen-2-yl)benzo[1,2-b:4,5-b′]dithiophene co-bipyridine polymer PCP4e (EQE$_{350\ nm}$ = 0.34%) and olefin-bridged

porous polymer OB-POP-3 ($EQE_{420 \, nm}$ = 2.0%) [198,199]. The crystallinity of TBAP-α decreases slowly with the progress of the reaction, and the hydrogen production rate also decreases, indicating that the photocatalytic performance of HOFs is closely related to its structure and crystallinity.
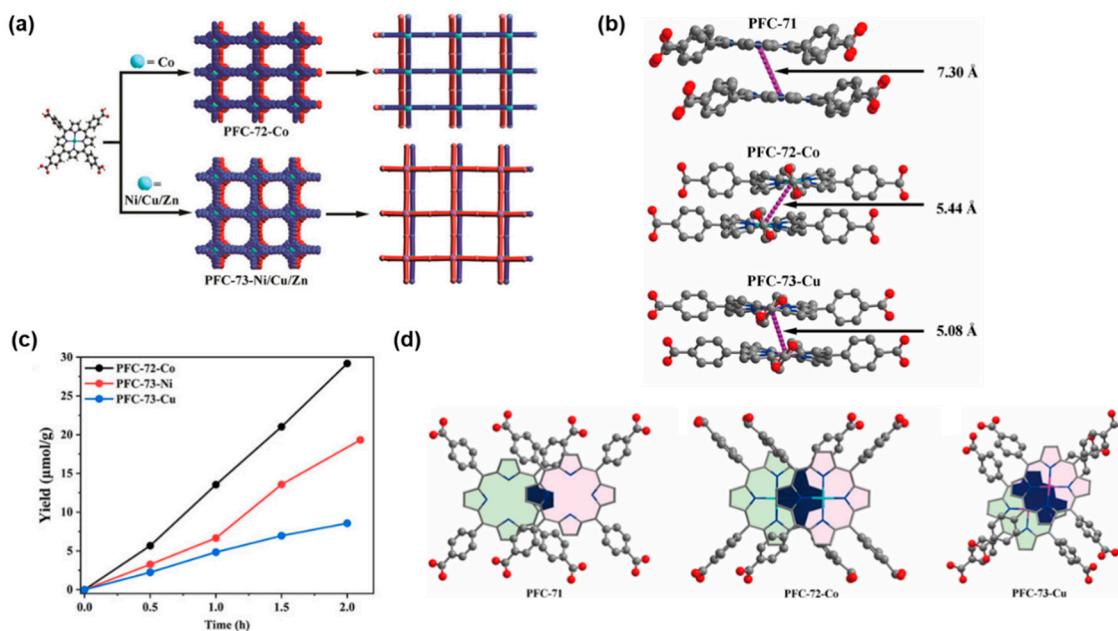

Figure 10. (**a**) Schematic representation of the construction of PFC-71, PFC-72-Co, and PFC-73-Ni/Cu/Zn; The offset π–π interactions of PFC-71, PFC-72-Co, and PFC-73-Cu viewed from the (010) plane (**b**) and the (−101) plane (**d**), showing interlayer porphyrin center-to-center distance and orbital overlap area highlighted in dark blue (hydrogen atoms are omitted for clarity); (**c**) Time-resolved CO productions of photocatalytic CO_2 reduction over PFC-72-Co, PFC-73-Ni, and PFC-73-Cu. Republish from Ref. [29], Copyright (2021), with permission from Wiley.

5.3.2. Degradation of Pollutants

The increasing pollutant wastewater has brought serious pollution to our environment, which is an urgent problem. Using photocatalysis to completely degrade organic pollutants into non-toxic molecules is considered to be an environmentally friendly and effective environmental protection strategy. HOFs, as emerging advanced crystalline porous materials, have recently been used to degrade these pollutants [38,200,201]. Shi et al. synthesized a novel Z-type PFC-1/CNNS heterojunction photocatalyst by in-situ electrostatic method to study the photocatalytic effect of methyl orange [38]. This Z-scheme heterojunction reduces the recombination probability of photogenerated holes and photogenerated electrons and accumulates more charge carriers to produce highly active substances (●O_2^-, ●OH, and h^+). In addition, the strong surface hydrophilicity of PFC-1/CNNS can weaken the interaction with water molecules and methyl orange (MO), and significantly improve the visible light catalytic performance. PFC-1/CNNS degraded 80% of MO after 30 min of light exposure, and completely degraded MO after 60 min. This study provides new implications for the photocatalytic degradation of pollutants by heterojunction materials.

The photocatalytic activity of 9,10-diphenylanthracene (DPA) degradation by meso-tetrakis(carboxylphenyl)porphyrin (TCPP)-based HOFs was studied [200]. TCPP-2 (DMF), TCPP-4 (DMF), and TCPP-6 (DMF) were obtained by blocking the "reverse strategy" of the strong hydrogen bond building unit on the main chain of TCPP to control the synthesis of HOF based on TCPP. The results showed that TCPP-6 (DMF) degraded 99% of DPA after 100 min of light exposure, while TCPP-2 (DMF) and TCPP-4 (DMF) required 120 and 150 min, respectively. More importantly, TCPP-6 (DMF) has excellent reusability in photocatalysis. These results indicate that the more DMF molecules bind, the greater the van der

Waals forces around TCPP molecules, and the higher the photostability and photocatalytic activity of TCPP-based HOF. Therefore, a positive correlation was established between the number of DMF molecules and the photocatalytic activity of porphyrinyl HOF, which would significantly promote the development of porphyrinyl photocatalytic materials.

5.4. Sensor Applications

In the presence of specific analytes, the luminescence properties of some luminous HOFs change (enhanced, quenched, or shifted), and the interaction between the material and the target analyte is analyzed by the luminescence changes. Effective sensing or detection of contaminants is essential before removal, even if the operation does not directly remove contaminants. HOFs are ideal sensing candidate materials because of their permanent porosity and high guest molecular load, which can improve the sensitivity of detection. HOFs are currently used to detect a variety of contaminants, including metal ions, anilines, salts, antibiotics, explosive vapors, and several other organic compounds [202–206].

Timely monitoring of trinitrotoluene (TNT), 2,4-dinitrotoluene (DNT), and other sensitive explosive vapors such as trinitrophenol (PA), trinitroresorcinol (TNR) is a top priority in heavy industry and scientific research institutions. The internal voids of the developed three-dimensional topological aggregates provide shelter for explosive vapors and exhibit extraordinary transmission with the help of coordinated complexation and electrostatic attraction. Therefore, as long as electron-rich aggregation-induced emission (AIE) hydrogen bond microporous skeleton pores adsorb electron-deficient nitroaromatics, the charge transfer between each other will quench the fluorescence AIE-HOF emission. The reaction of three tetraphenylethylene-based fluorescent single crystals TPE-AA-1, 2, 3 (TPE = tetraphenylethylene) based on tetraphenylvinyl to nitroaromatics was studied [206]. For TPE-AA-3, the quenching efficiency reaches 90.9%. This is because TPE-AA-3 has a greater BET than the other two, and tends to adhere to nitro aromatic groups, so it shows obvious fluorescence quenching.

Most sensing processes for environmentally relevant species take place in water, where HOF sensors are a challenging feature. Tang and his colleagues synthesized POSS-T_8A (POSS = polyhedral oligomeric silsesquioxane), by a condensation reaction based on an AIE precursor and a siloxane derivative [33]. It was found that it showed high sensitivity to Cu^{2+} ions and fluorescence quenching selectivity. The selectivity is attributed to the ability of the amide bond in HOF to bind to the Cu^{2+} ion, which causes the conformational change of the luminogen tetraphenylethene (TPE) unit in POSS-T_8A, leading to fluorescence quenching. The fluorescence amplification of HOF-20 for aniline in water was studied [207]. The detection limit was 2.24 μM, and the influence of other aromatic interference on its detection performance was negligible. Aniline molecules in HOF-20 will form multiple intermolecular interactions with the skeleton and may restrict the torsional rotation of aromatic rings in the connectome. This limitation can reduce the non-radiative attenuation path after photoexcitation, resulting in the fluorescence attenuation of HOF-20. Zhu et al. prepared Eu^{3+} functionalized HOF(Eu@HOF-GS-10) by ion exchange between Eu^{3+} ions and guanidine cations [205]. Eu@HOF-GS-10 shows a distinct red fluorescence, which can quickly respond to eight quinolones using machine learning (ML) to analyze and process the data.

6. Conclusions

HOFs as a new crystalline porous polymer have attracted extensive attention. Due to their remarkable properties of metal-free, high stability, high surface area, easily adjustable pore size, and easy regeneration and recovery, HOFs show great potential in the field of environmental remediation, including gas adsorption and separation (NH_3, CO_2/CH_4, and CO_2/N_2, C_2H_2/C_2H_4 and C_2H_4/C_2H_6, C_2H_2/CO_2, Xe/Kr, etc.), heavy metals and radioactive metals adsorption, organic dyes and pesticides adsorption, energy conversion (production of H_2 and CO_2 reduction to CO), degradation of organic dyes, and contaminants sensing (metal ions, anilines, antibiotics, explosive vapors, etc.). However, due to

their slow development compared with other porous materials and complex chemistry, the application of HOFs in environmental remediation is still in its infancy, and there are still many problems to be solved.

1. Functionalization brings additional functionality to the HOFs' holes. Due to the periodic network chemical structure of HOFs, different functional groups, such as aromatic and aliphatic groups, esters, carboxylic acids, and alcohols, can be selected to pre-design the structure of HOFs, so as to achieve the purpose of precise regulation of its structure and properties. Various functional groups allow HOFs to be applied in specific areas, such as increasing the interaction of HOFs with pollutants to remove them from gases or solutions;

2. With the development of computer technology, molecular simulation technology has been widely used in the mechanism study of some materials, which can not only clarify the interaction between adsorbent and adsorption sites on the inner surface of adsorbent channels qualitatively, but also obtain quantitative results. Compared with traditional experimental methods, molecular simulation has the advantages of convenience and speed, and can obtain microscopic information which is difficult to obtain in conventional experiments. Therefore, molecular simulation technology can be hoped to screen whether HOFs have adsorption properties for specific pollutants, and explain the adsorption mechanism at the molecular level;

3. HOFs need to be extended beyond traditional water and air pollution to cover new frontiers, such as the remediation of contaminated land (soil). Remediation of contaminated soil is an urgent environmental problem. If not dealt with effectively, it will seriously destroy the whole ecosystem and endanger human health through the biological chain. HOFs can be used to separate pollutants from the soil by adsorption, or reduce pollutants to dissoluble states by chemical reducing agents, thus reducing the migration and bioavailability of pollutants in the soil environment;

4. Through DFT high-throughput computing and machine learning, we hoped to build predictive single objective/multi-objective nature-oriented HOFs intelligent platforms to develop low-cost and efficient HOFs to remove pollutants from the environment and facilitate their large-scale application.

With the rapid development of HOFs, the application of HOFs in environmental remediation has shown great prospects. Although there are still some challenges, we believe that more interesting and attractive multifunctional material platforms can be built in the near future to realize their full potential.

Author Contributions: Data curation, Writing—Original draft preparation, and Investigation, Y.Z. and M.T.; Writing—Review and Editing, Z.M.; Visualization and Investigation, Y.X.; Resources and Investigation, K.Z.; Formal analysis, Z.L.; Resources, C.L.; Supervision and Project administration, C.Z. All authors have read and agreed to the published version of the manuscript.

Data Availability Statement: Not applicable.

Conflicts of Interest: The authors confirm that this article's content has no conflict of interest.

References

1. Ong, W.-J.; Tan, L.-L.; Ng, Y.H.; Yong, S.-T.; Chai, S.-P. Graphitic Carbon Nitride (g-C$_3$N$_4$)-Based Photocatalysts for Artificial Photosynthesis and Environmental Remediation: Are We a Step Closer To Achieving Sustainability? *Chem. Rev.* **2016**, *116*, 7159–7329. [CrossRef]
2. Wang, H.; Li, X.; Zhao, X.; Li, C.; Song, X.; Zhang, P.; Huo, P. A review on heterogeneous photocatalysis for environmental remediation: From semiconductors to modification strategies. *Chin. J. Catal.* **2022**, *43*, 178–214. [CrossRef]

3. Chakraborty, J.; Nath, I.; Song, S.; Mohamed, S.; Khan, A.; Heynderickx, P.M.; Verpoort, F. Porous organic polymer composites as surging catalysts for visible-light-driven chemical transformations and pollutant degradation. *J. Photochem. Photobiol. C Photochem. Rev.* **2019**, *41*, 100319. [CrossRef]

4. Rasheed, T. Covalent organic frameworks as promising adsorbent paradigm for environmental pollutants from aqueous matrices: Perspective and challenges. *Sci. Total Environ.* **2022**, *833*, 155279. [CrossRef] [PubMed]

5. Musarurwa, H.; Tavengwa, N.T. Smart metal-organic framework (MOF) composites and their applications in environmental remediation. *Mater. Today Commun.* **2022**, *33*, 104823. [CrossRef]

6. Lin, R.-B.; Chen, B. Hydrogen-bonded organic frameworks: Chemistry and functions. *Chem* **2022**, *8*, 2114–2135. [CrossRef]

7. Yu, B.; Liu, Y.; Li, Z.; Liu, Y.; Rao, P.; Li, G. Durable substrates incorporated with MOFs: Recent advances in engineering strategies and water treatment applications. *Chem. Eng. J.* **2023**, *455*, 140840. [CrossRef]

8. Patial, S.; Soni, V.; Kumar, A.; Raizada, P.; Ahamad, T.; Pham, X.M.; van Le, Q.; Nguyen, V.-H.; Thakur, S.; Singh, P. Rational design, structure properties, and synthesis strategies of dual-pore covalent organic frameworks (COFs) for potent applications: A review. *Environ. Res.* **2023**, *218*, 114982. [CrossRef]

9. Thorarinsdottir, A.E.; Harris, T.D. Metal-Organic Framework Magnets. *Chem. Rev.* **2020**, *120*, 8716–8789. [CrossRef] [PubMed]

10. Gaillac, R.; Pullumbi, P.; Beyer, K.A.; Chapman, K.W.; Keen, D.A.; Bennett, T.D.; Coudert, F.-X. Liquid metal-organic frameworks. *Nat. Mater.* **2017**, *16*, 1149–1154. [CrossRef] [PubMed]

11. Xia, C.; Kirlikovali, K.O.; Nguyen, T.H.C.; Nguyen, X.C.; Tran, Q.B.; Duong, M.K.; Nguyen Dinh, M.T.; Le Nguyen, D.T.; Singh, P.; Raizada, P.; et al. The emerging covalent organic frameworks (COFs) for solar-driven fuels production. *Coord. Chem. Rev.* **2021**, *446*, 214117. [CrossRef]

12. Wu, Y.; Mao, X.; Zhang, M.; Zhao, X.; Xue, R.; Di, S.; Huang, W.; Wang, L.; Li, Y.; Li, Y. 2D Molecular Sheets of Hydrogen-Bonded Organic Frameworks for Ultrastable Sodium-Ion Storage. *Adv. Mater.* **2021**, *33*, e2106079. [CrossRef] [PubMed]

13. Hisaki, I.; Suzuki, Y.; Gomez, E.; Cohen, B.; Tohnai, N.; Douhal, A. Docking Strategy To Construct Thermostable, Single-Crystalline, Hydrogen-Bonded Organic Framework with High Surface Area. *Angew. Chem. Int. Ed. Engl.* **2018**, *57*, 12650–12655. [CrossRef]

14. Xu, X.-Q.; Cao, L.-H.; Yang, Y.; Zhao, F.; Bai, X.-T.; Zang, S.-Q. Hybrid Nafion Membranes of Ionic Hydrogen-Bonded Organic Framework Materials for Proton Conduction and PEMFC Applications. *ACS Appl. Mater. Interfaces* **2021**, *13*, 56566–56574. [CrossRef] [PubMed]

15. Wang, B.; Lin, R.-B.; Zhang, Z.; Xiang, S.; Chen, B. Hydrogen-Bonded Organic Frameworks as a Tunable Platform for Functional Materials. *J. Am. Chem. Soc.* **2020**, *142*, 14399–14416. [CrossRef]

16. Khadivjam, T.; Che-Quang, H.; Maris, T.; Ajoyan, Z.; Howarth, A.J.; Wuest, J.D. Modular Construction of Porous Hydrogen-Bonded Molecular Materials from Melams. *Chemistry* **2020**, *26*, 7026–7040. [CrossRef] [PubMed]

17. Duchamp, D.J.; Marsh, R.E. The crystal structure of trimesic acid (benzene-1,3,5-tricarboxylic acid). *Acta Crystallogr. B Struct. Crystallogr. Cryst. Chem.* **1969**, *25*, 5–19. [CrossRef]

18. Simard, M.; Su, D.; Wuest, J.D. Use of hydrogen bonds to control molecular aggregation. Self-assembly of three-dimensional networks with large chambers. *J. Am. Chem. Soc.* **1991**, *113*, 4696–4698. [CrossRef]

19. Brunet, P.; Simard, M.; Wuest, J.D. Molecular Tectonics. Porous Hydrogen-Bonded Networks with Unprecedented Structural Integrity. *J. Am. Chem. Soc.* **1997**, *119*, 2737–2738. [CrossRef]

20. Saied, O.; Maris, T.; Simard, M.; Wuest, J.D. Tetrakis(3,5-dimethoxyphenyl)silane. *Acta Crystallogr. E Struct. Rep. Online* **2005**, *61*, o2563–o2566. [CrossRef]

21. Fournier, J.-H.; Maris, T.; Wuest, J.D. Molecular tectonics. Porous hydrogen-bonded networks built from derivatives of 9,9′-spirobifluorene. *J. Org. Chem.* **2004**, *69*, 1762–1775. [CrossRef]

22. He, Y.; Xiang, S.; Chen, B. A microporous hydrogen-bonded organic framework for highly selective C_2H_2/C_2H_4 separation at ambient temperature. *J. Am. Chem. Soc.* **2011**, *133*, 14570–14573. [CrossRef]

23. Lin, R.-B.; He, Y.; Li, P.; Wang, H.; Zhou, W.; Chen, B. Multifunctional porous hydrogen-bonded organic framework materials. *Chem. Soc. Rev.* **2019**, *48*, 1362–1389. [CrossRef] [PubMed]

24. Yang, J.; Wang, J.; Hou, B.; Huang, X.; Wang, T.; Bao, Y.; Hao, H. Porous hydrogen-bonded organic frameworks (HOFs): From design to potential applications. *Chem. Eng. J.* **2020**, *399*, 125873. [CrossRef]

25. Ding, X.; Liu, Z.; Zhang, Y.; Ye, G.; Jia, J.; Chen, J. Binary Solvent Regulated Architecture of Ultra-Microporous Hydrogen-Bonded Organic Frameworks with Tunable Polarization for Highly-Selective Gas Separation. *Angew. Chem. Int. Ed. Engl.* **2022**, *61*, e202116483. [CrossRef]

26. Gao, J.; Cai, Y.; Qian, X.; Liu, P.; Wu, H.; Zhou, W.; Liu, D.-X.; Li, L.; Lin, R.-B.; Chen, B. A Microporous Hydrogen-Bonded Organic Framework for the Efficient Capture and Purification of Propylene. *Angew. Chem. Int. Ed. Engl.* **2021**, *60*, 20400–20406. [CrossRef]

27. Liu, P.-D.; Liu, A.-G.; Wang, P.-M.; Chen, Y.; Li, B. Smart crystalline frameworks constructed with bisquinoxaline-based component for multi-stimulus luminescent sensing materials. *Chin. J. Struct. Chem.* **2022**, *41*, 100001. [CrossRef]

28. Yang, Z.; Zhang, Y.; Wu, W.; Zhou, Z.; Gao, H.; Wang, J.; Jiang, Z. Hydrogen-bonded organic framework membrane with efficient proton conduction. *J. Membr. Sci.* **2022**, *664*, 121118. [CrossRef]

29. Yin, Q.; Alexandrov, E.V.; Si, D.-H.; Huang, Q.-Q.; Fang, Z.-B.; Zhang, Y.; Zhang, A.-A.; Qin, W.-K.; Li, Y.-L.; Liu, T.-F.; et al. Metallization-Prompted Robust Porphyrin-Based Hydrogen-Bonded Organic Frameworks for Photocatalytic CO_2 Reduction. *Angew. Chem. Int. Ed. Engl.* **2022**, *61*, e202115854. [CrossRef] [PubMed]

30. Liang, W.; Carraro, F.; Solomon, M.B.; Bell, S.G.; Amenitsch, H.; Sumby, C.J.; White, N.G.; Falcaro, P.; Doonan, C.J. Enzyme Encapsulation in a Porous Hydrogen-Bonded Organic Framework. *J. Am. Chem. Soc.* **2019**, *141*, 14298–14305. [CrossRef]

31. Zhang, N.; Yin, Q.; Guo, S.; Chen, K.-K.; Liu, T.-F.; Wang, P.; Zhang, Z.-M.; Lu, T.-B. Hot-electron leading-out strategy for constructing photostable HOF catalysts with outstanding H2 evolution activity. *Appl. Catal. B Environ.* **2021**, *296*, 120337. [CrossRef]

32. Luo, X.-Z.; Jia, X.-J.; Deng, J.-H.; Zhong, J.-L.; Liu, H.-J.; Wang, K.-J.; Zhong, D.-C. A microporous hydrogen-bonded organic framework: Exceptional stability and highly selective adsorption of gas and liquid. *J. Am. Chem. Soc.* **2013**, *135*, 11684–11687. [CrossRef] [PubMed]

33. Zhou, H.; Ye, Q.; Wu, X.; Song, J.; Cho, C.M.; Zong, Y.; Tang, B.Z.; Hor, T.S.A.; Yeow, E.K.L.; Xu, J. A thermally stable and reversible microporous hydrogen-bonded organic framework: Aggregation induced emission and metal ion-sensing properties. *J. Mater. Chem. C* **2015**, *3*, 11874–11880. [CrossRef]

34. Lu, Y.; Yu, K.; Yin, Q.; Liu, J.; Han, X.; Zhao, D.; Liu, T.; Li, C. Embedding red-emitting dyes in robust hydrogen-bonded organic framework for application in warm white light-emitting diodes. *Microporous Mesoporous Mater.* **2022**, *331*, 111673. [CrossRef]

35. Han, B.; Wang, H.; Wang, C.; Wu, H.; Zhou, W.; Chen, B.; Jiang, J. Postsynthetic Metalation of a Robust Hydrogen-Bonded Organic Framework for Heterogeneous Catalysis. *J. Am. Chem. Soc.* **2019**, *141*, 8737–8740. [CrossRef]

36. Wang, H.; Li, B.; Wu, H.; Hu, T.-L.; Yao, Z.; Zhou, W.; Xiang, S.; Chen, B. A Flexible Microporous Hydrogen-Bonded Organic Framework for Gas Sorption and Separation. *J. Am. Chem. Soc.* **2015**, *137*, 9963–9970. [CrossRef]

37. Liu, J.; Li, L.; Niu, W.; Wang, N.; Zhao, D.; Zeng, S.; Chen, S. A Hydrogen-Bonded Organic-Framework-Derived Mesoporous N-Doped Carbon for Efficient Electroreduction of Oxygen. *ChemElectroChem* **2016**, *3*, 1116–1123. [CrossRef]

38. Shi, H.; Feng, D.; Li, H.; Yu, D.; Chen, X. Hydrophilic hydrogen-bonded organic frameworks/g-C$_3$N$_4$ all-organic Z-scheme heterojunction for efficient visible-light photocatalytic hydrogen production and dye degradation. *J. Photochem. Photobiol. A Chem.* **2023**, *435*, 114292. [CrossRef]

39. Liu, Y.; Xu, X.; Lu, H.; Yan, B. Dual-emission ratiometric fluorescent probe-based lanthanide-functionalized hydrogen-bonded organic framework for the visual detection of methylamine. *J. Mater. Chem. C* **2022**, *10*, 1212–1219. [CrossRef]

40. Zhu, Z.-H.; Wang, H.-L.; Zou, H.-H.; Liang, F.-P. Metal hydrogen-bonded organic frameworks: Structure and performance. *Dalton Trans.* **2020**, *49*, 10708–10723. [CrossRef]

41. Yan, L.; Li, C.; Chen, X. Hydrogen bonded supra-molecular framework in inorganic–organic hybrid compounds of Mn(II) and Zn(II): Syntheses, structures, and photoluminescent studies. *J. Mol. Struct.* **2014**, *1058*, 277–283. [CrossRef]

42. Kanetomo, T.; Ni, Z.; Enomoto, M. Hydrogen-bonded cobalt(II)-organic framework: Normal and reverse spin-crossover behaviours. *Dalton Trans.* **2022**, *51*, 5034–5040. [CrossRef]

43. Werner, T.W.; Reschke, S.; Bunzen, H.; von Nidda, H.-A.K.; Deisenhofer, J.; Loidl, A.; Volkmer, D. Co5Tp*4(Me2bta)6: A Highly Symmetrical Pentanuclear Kuratowski Complex Featuring Tris(pyrazolyl)borate and Benzotriazolate Ligands. *Inorg. Chem.* **2016**, *55*, 1053–1060. [CrossRef]

44. Lin, T.; Sun, Y.; Tian, C.; Wang, D.; Hou, L.; Ye, F.; Zhao, S. A silk-like hydrogen-bonded organic framework functionalized membrane with intrinsic catalytic activity for nonmetallic reduction of 4-nitrophenol. *Chem. Eng. J.* **2022**, *441*, 136092. [CrossRef]

45. Song, Q.; Xu, D.; David Wang, W.; Fang, J.; Sun, X.; Li, F.; Li, B.; Kou, J.; Zhu, H.; Dong, Z. Ru clusters confined in Hydrogen-bonded organic frameworks for homogeneous catalytic hydrogenation of N-heterocyclic compounds with heterogeneous recyclability. *J. Catal.* **2022**, *406*, 19–27. [CrossRef]

46. Hou, X.; Wang, Z.; Overby, M.; Ugrinov, A.; Oian, C.; Singh, R.; Chu, Q.R. A two-dimensional hydrogen bonded organic framework self-assembled from a three-fold symmetric carbamate. *Chem. Commun.* **2014**, *50*, 5209–5211. [CrossRef] [PubMed]

47. Lin, Z.-J.; Mahammed, S.A.R.; Liu, T.-F.; Cao, R. Multifunctional Porous Hydrogen-Bonded Organic Frameworks: Current Status and Future Perspectives. *ACS Cent. Sci.* **2022**, *8*, 1589–1608. [CrossRef] [PubMed]

48. Li, P.; He, Y.; Guang, J.; Weng, L.; Zhao, J.C.-G.; Xiang, S.; Chen, B. A homochiral microporous hydrogen-bonded organic framework for highly enantioselective separation of secondary alcohols. *J. Am. Chem. Soc.* **2014**, *136*, 547–549. [CrossRef]

49. Nicks, J.; Boer, S.A.; White, N.G.; Foster, J.A. Monolayer nanosheets formed by liquid exfoliation of charge-assisted hydrogen-bonded frameworks. *Chem. Sci.* **2021**, *12*, 3322–3327. [CrossRef]

50. Mastalerz, M.; Oppel, I.M. Rational construction of an extrinsic porous molecular crystal with an extraordinary high specific surface area. *Angew. Chem. Int. Ed. Engl.* **2012**, *51*, 5252–5255. [CrossRef]

51. Hashim, M.I.; Le, H.T.M.; Chen, T.-H.; Chen, Y.-S.; Daugulis, O.; Hsu, C.-W.; Jacobson, A.J.; Kaveevivitchai, W.; Liang, X.; Makarenko, T.; et al. Dissecting Porosity in Molecular Crystals: Influence of Geometry, Hydrogen Bonding, and π···π Stacking on the Solid-State Packing of Fluorinated Aromatics. *J. Am. Chem. Soc.* **2018**, *140*, 6014–6026. [CrossRef] [PubMed]

52. Li, Y.-L.; Alexandrov, E.V.; Yin, Q.; Li, L.; Fang, Z.-B.; Yuan, W.; Proserpio, D.M.; Liu, T.-F. Record Complexity in the Polycatenation of Three Porous Hydrogen-Bonded Organic Frameworks with Stepwise Adsorption Behaviors. *J. Am. Chem. Soc.* **2020**, *142*, 7218–7224. [CrossRef] [PubMed]

53. Hu, F.; Liu, C.; Wu, M.; Pang, J.; Jiang, F.; Yuan, D.; Hong, M. An Ultrastable and Easily Regenerated Hydrogen-Bonded Organic Molecular Framework with Permanent Porosity. *Angew. Chem. Int. Ed. Engl.* **2017**, *56*, 2101–2104. [CrossRef] [PubMed]

54. Liu, X.; Yang, X.; Wang, H.; Hisaki, I.; Wang, K.; Jiang, J. A robust redox-active hydrogen-bonded organic framework for rechargeable batteries. *J. Mater. Chem. A* **2022**, *10*, 1808–1814. [CrossRef]

55. Yang, W.; Wang, J.; Wang, H.; Bao, Z.; Zhao, J.C.-G.; Chen, B. Highly Interpenetrated Robust Microporous Hydrogen-Bonded Organic Framework for Gas Separation. *Cryst. Growth Des.* **2017**, *17*, 6132–6137. [CrossRef]

56. Malek, N.; Maris, T.; Perron, M.-E.; Wuest, J.D. Molecular tectonics: Porous cleavable networks constructed by dipole-directed stacking of hydrogen-bonded sheets. *Angew. Chem. Int. Ed. Engl.* **2005**, *44*, 4021–4025. [CrossRef]

57. Malek, N.; Maris, T.; Simard, M.; Wuest, J.D. Molecular tectonics. Selective exchange of cations in porous anionic hydrogen-bonded networks built from derivatives of tetraphenylborate. *J. Am. Chem. Soc.* **2005**, *127*, 5910–5916. [CrossRef]

58. Beijer, F.H.; Sijbesma, R.P.; Vekemans, J.A.J.M.; Meijer, E.W.; Kooijman, H.; Spek, A.L. Hydrogen-Bonded Complexes of Diaminopyridines and Diaminotriazines: Opposite Effect of Acylation on Complex Stabilities. *J. Org. Chem.* **1996**, *61*, 9636. [CrossRef]

59. Hisaki, I.; Xin, C.; Takahashi, K.; Nakamura, T. Designing Hydrogen-Bonded Organic Frameworks (HOFs) with Permanent Porosity. *Angew. Chem. Int. Ed. Engl.* **2019**, *58*, 11160–11170. [CrossRef]

60. Yu, B.; Geng, S.; Wang, H.; Zhou, W.; Zhang, Z.; Chen, B.; Jiang, J. A Solid Transformation into Carboxyl Dimers Based on a Robust Hydrogen-Bonded Organic Framework for Propyne/Propylene Separation. *Angew. Chem. Int. Ed. Engl.* **2021**, *60*, 25942–25948. [CrossRef]

61. Russell, V.A.; Etter, M.C.; Ward, M.D. Layered Materials by Molecular Design: Structural Enforcement by Hydrogen Bonding in Guanidinium Alkane- and Arenesulfonates. *J. Am. Chem. Soc.* **1994**, *116*, 1941–1952. [CrossRef]

62. Kang, D.W.; Kang, M.; Kim, H.; Choe, J.H.; Kim, D.W.; Park, J.R.; Lee, W.R.; Moon, D.; Hong, C.S. A Hydrogen-Bonded Organic Framework (HOF) with Type IV NH_3 Adsorption Behavior. *Angew. Chem. Int. Ed. Engl.* **2019**, *58*, 16152–16155. [CrossRef] [PubMed]

63. Luo, Y.-H.; He, X.-T.; Hong, D.-L.; Chen, C.; Chen, F.-H.; Jiao, J.; Zhai, L.-H.; Guo, L.-H.; Sun, B.-W. A Dynamic 3D Hydrogen-Bonded Organic Frameworks with Highly Water Affinity. *Adv. Funct. Mater.* **2018**, *28*, 1804822. [CrossRef]

64. Zheng, X.; Xiao, N.; Long, Z.; Wang, L.; Ye, F.; Fang, J.; Shen, L.; Xiao, X. Hydrogen bonded-directed pure organic frameworks based on TTF-tetrabenzoic acid and bipyridine base. *Synth. Met.* **2020**, *263*, 116365. [CrossRef]

65. Lü, J.; Perez-Krap, C.; Suyetin, M.; Alsmail, N.H.; Yan, Y.; Yang, S.; Lewis, W.; Bichoutskaia, E.; Tang, C.C.; Blake, A.J.; et al. A robust binary supramolecular organic framework (SOF) with high CO_2 adsorption and selectivity. *J. Am. Chem. Soc.* **2014**, *136*, 12828–12831. [CrossRef] [PubMed]

66. Ahmed, I.; Mondol, M.M.H.; Lee, H.J.; Jhung, S.H. Application of Metal-Organic Frameworks in Adsorptive Removal of Organic Contaminants from Water, Fuel and Air. *Chem. Asian J.* **2021**, *16*, 185–196. [CrossRef]

67. Mondol, M.M.H.; Bhadra, B.N.; Jhung, S.H. Molybdenum nitride@porous carbon, derived from phosphomolybdic acid loaded metal-azolate framework-6: A highly effective catalyst for oxidative desulfurization. *Appl. Catal. B Environ.* **2021**, *288*, 119988. [CrossRef]

68. Bhadra, B.N.; Baek, Y.S.; Kim, S.; Choi, C.H.; Jhung, S.H. Oxidative denitrogenation of liquid fuel over W2N@carbon catalyst derived from a phosphotungstinic acid encapsulated metal–azolate framework. *Appl. Catal. B Environ.* **2021**, *285*, 119842. [CrossRef]

69. Diskin-Posner, Y.; Krishna Kumar, R.; Goldberg, I. Solid-state supramolecular chemistry of porphyrins. Stacked and layered heterogeneous aggregation modes of tetraarylporphyrins with crown ethers. *New J. Chem.* **1999**, *23*, 885–890. [CrossRef]

70. Zhang, Z.; Duan, Y.; Zhang, L.; Yu, M.; Li, J. Synthesis, crystal structure of two new Zn(II), Cu(II) porphyrins and their catalytic activities to ethylbenzene oxidation. *Inorg. Chem. Commun.* **2015**, *58*, 53–56. [CrossRef]

71. Taylor, J.M.; Dwyer, P.J.; Reid, J.W.; Gelfand, B.S.; Lim, D.-W.; Donoshita, M.; Veinberg, S.L.; Kitagawa, H.; Vukotic, V.N.; Shimizu, G.K.H. Holding Open Micropores with Water: Hydrogen-Bonded Networks Supported by Hexaaquachromium(III) Cations. *Chem* **2018**, *4*, 868–878. [CrossRef]

72. Wang, X.-Y.; Justice, R.; Sevov, S.C. Hydrogen-bonded metal-complex sulfonate (MCS) inclusion compounds: Effect of the guest molecule on the host framework. *Inorg. Chem.* **2007**, *46*, 4626–4631. [CrossRef]

73. Wang, X.-Y.; Sevov, S.C. Hydrogen-Bonded Host Frameworks of Cationic Metal Complexes and Anionic Disulfonate Linkers: Effects of the Guest Molecules and the Charge of the Metal Complex. *Chem. Mater.* **2007**, *19*, 4906–4912. [CrossRef]

74. Wang, X.-Y.; Sevov, S.C. A Series of Guest-Defined Metal-Complex/Disulfonate Frameworks of Hydrogen-Bonded [Co(en) 2 (ox)] + and 2,6-Naphtalenedisulfonate. *Cryst. Growth Des.* **2008**, *8*, 1265–1270. [CrossRef]

75. Dalrymple, S.A.; Shimizu, G.K.H. Second-sphere coordination networks: 'Tame-ing' (Tame=1,1,1-Tris(aminomethyl)ethane) the hydrogen bond. *J. Mol. Struct.* **2006**, *796*, 95–106. [CrossRef]

76. Chand, S.; Pal, S.C.; Pal, A.; Ye, Y.; Lin, Q.; Zhang, Z.; Xiang, S.; Das, M.C. Metalo Hydrogen-Bonded Organic Frameworks (MHOFs) as New Class of Crystalline Materials for Protonic Conduction. *Chemistry* **2019**, *25*, 1691–1695. [CrossRef] [PubMed]

77. Zhang, H.-X.; Yan, X.; Chen, Y.-X.; Zhang, S.-H.; Li, T.; Han, W.-K.; Bao, L.-Y.; Shen, R.; Gu, Z.-G. A zeolite supramolecular framework with LTA topology based on a tetrahedral metal-organic cage. *Chem. Commun.* **2019**, *55*, 1120–1123. [CrossRef] [PubMed]

78. Luo, D.; Zhou, X.-P.; Li, D. Beyond molecules: Mesoporous supramolecular frameworks self-assembled from coordination cages and inorganic anions. *Angew. Chem. Int. Ed. Engl.* **2015**, *54*, 6190–6195. [CrossRef]

79. Ferlay, S.; Hellwig, P.; Wais Hosseini, M. Partially Reversible Thermal-Induced Oxidation During a Dehydration Process in an H-bonded Supramolecular System. *Chemphyschem* **2018**, *19*, 3219–3225. [CrossRef]

80. Mouchaham, G.; Roques, N.; Khodja, W.; Duhayon, C.; Coppel, Y.; Brandès, S.; Fodor, T.; Meyer, M.; Sutter, J.-P. Hydrogen-Bonded Open-Framework with Pyridyl-Decorated Channels: Straightforward Preparation and Insight into Its Affinity for Acidic Molecules in Solution. *Chemistry* **2017**, *23*, 11818–11826. [CrossRef]

81. Yokomori, S.; Ueda, A.; Higashino, T.; Kumai, R.; Murakami, Y.; Mori, H. Construction of three-dimensional anionic molecular frameworks based on hydrogen-bonded metal dithiolene complexes and the crystal solvent effect. *CrystEngComm* **2019**, *21*, 2940–2948. [CrossRef]

82. Beach, G.J.; Hogan, C.E.; Besong, B.N.; Hogan, G.A. Inclusion of alkyl alcohol guest molecules into a copper (II)-based hydrogen-bonded metal-organic framework. *J. Mol. Struct.* **2019**, *1195*, 744–746. [CrossRef]

83. Shao, D.; Peng, P.; You, M.; Shen, L.-F.; She, S.-Y.; Zhang, Y.-Q.; Tian, Z. Hydrogen-Bonded Framework of a Cobalt(II) Complex Showing Superior Stability and Field-Induced Slow Magnetic Relaxation. *Inorg. Chem.* **2022**, *61*, 3754–3762. [CrossRef]

84. Alrefai, A.; Mondal, S.S.; Wruck, A.; Kelling, A.; Schilde, U.; Brandt, P.; Janiak, C.; Schönfeld, S.; Weber, B.; Rybakowski, L.; et al. Hydrogen-bonded supramolecular metal-imidazolate frameworks: Gas sorption, magnetic and UV/Vis spectroscopic properties. *J. Incl. Phenom. Macrocycl. Chem.* **2019**, *94*, 155–165. [CrossRef]

85. Tholen, P.; Peeples, C.A.; Ayhan, M.M.; Wagner, L.; Thomas, H.; Imbrasas, P.; Zorlu, Y.; Baretzky, C.; Reineke, S.; Hanna, G.; et al. Tuning Structural and Optical Properties of Porphyrin-based Hydrogen-Bonded Organic Frameworks by Metal Insertion. *Small* **2022**, *18*, e2204578. [CrossRef]

86. Zhang, A.-A.; Si, D.; Huang, H.; Xie, L.; Fang, Z.-B.; Liu, T.-F.; Cao, R. Partial Metalation of Porphyrin Moieties in Hydrogen-Bonded Organic Frameworks Provides Enhanced CO_2 Photoreduction Activity. *Angew. Chem. Int. Ed. Engl.* **2022**, *61*, e202203955. [CrossRef]

87. Zhang, A.-A.; Li, Y.-L.; Fang, Z.-B.; Xie, L.; Cao, R.; Liu, Y.; Liu, T.-F. Facile Preparation of Hydrogen-Bonded Organic Framework/Cu2O Heterostructure Films via Electrophoretic Deposition for Efficient CO_2 Photoreduction. *ACS Appl. Mater. Interfaces* **2022**, *14*, 21050–21058. [CrossRef]

88. Liu, B.-T.; Pan, X.-H.; Zhang, D.-Y.; Wang, R.; Chen, J.-Y.; Fang, H.-R.; Liu, T.-F. Construction of Function-Oriented Core-Shell Nanostructures in Hydrogen-Bonded Organic Frameworks for Near-Infrared-Responsive Bacterial Inhibition. *Angew. Chem. Int. Ed. Engl.* **2021**, *60*, 25701–25707. [CrossRef] [PubMed]

89. Li, W.; Li, Y.; Caro, J.; Huang, A. Fabrication of a flexible hydrogen-bonded organic framework based mixed matrix membrane for hydrogen separation. *J. Membr. Sci.* **2022**, *643*, 120021. [CrossRef]

90. Liu, J.; Li, W.; Chen, H.; Li, S.; Yang, L.; Peng, K.; Cai, C.; Huang, X. Applications of functional nanoparticle–stabilized surfactant foam in petroleum-contaminated soil remediation. *J. Hazard. Mater.* **2023**, *443*, 130267. [CrossRef]

91. Mathur, J.; Goswami, P.; Gupta, A.; Srivastava, S.; Minkina, T.; Shan, S.; Rajput, V.D. Nanomaterials for Water Remediation: An Efficient Strategy for Prevention of Metal(loid) Hazard. *Water* **2022**, *14*, 3998. [CrossRef]

92. Wang, C.; Wang, Y.; Kirlikovali, K.O.; Ma, K.; Zhou, Y.; Li, P.; Farha, O.K. Ultrafine Silver Nanoparticle Encapsulated Porous Molecular Traps for Discriminative Photoelectrochemical Detection of Mustard Gas Simulants by Synergistic Size-Exclusion and Site-Specific Recognition. *Adv. Mater.* **2022**, *34*, e2202287. [CrossRef]

93. Bhadra, B.N.; Yoo, D.K.; Jhung, S.H. Carbon-derived from metal-organic framework MOF-74: A remarkable adsorbent to remove a wide range of contaminants of emerging concern from water. *Appl. Surf. Sci.* **2020**, *504*, 144348. [CrossRef]

94. Wang, L.; Yang, Y.; Liang, H.; Wu, N.; Peng, X.; Wang, L.; Song, Y. A novel N,S-rich COF and its derived hollow N,S-doped carbon@Pd nanorods for electrochemical detection of Hg2+ and paracetamol. *J. Hazard. Mater.* **2021**, *409*, 124528. [CrossRef] [PubMed]

95. Guo, Y.; Sun, Q.; Huang, Q.; Hu, Y.; Su, K.; Li, T.-T.; Huang, S.; Qian, J. Variable HOF-derived carbon-coated cobalt phosphide for electrocatalytic oxygen evolution. *Carbon* **2022**, *196*, 457–465. [CrossRef]

96. Liu, W.-J.; Wen, Y.-Q.; Wang, J.-W.; Zhong, D.-C.; Tan, J.-B.; Lu, T.-B. Nitrogen- and iodine-doped microporous carbon derived from a hydrogen-bonded organic framework: An efficient metal-free electrocatalyst for the oxygen reduction reaction. *J. Mater. Chem. A* **2019**, *7*, 9587–9592. [CrossRef]

97. Hu, H.; Han, L.; Yu, M.; Wang, Z.; Lou, X.W. Metal–organic-framework-engaged formation of Co nanoparticle-embedded carbon@Co9S8 double-shelled nanocages for efficient oxygen reduction. *Energy Environ. Sci.* **2016**, *9*, 107–111. [CrossRef]

98. Zhang, S.; Xia, W.; Yang, Q.; Valentino Kaneti, Y.; Xu, X.; Alshehri, S.M.; Ahamad, T.; Hossain, M.S.A.; Na, J.; Tang, J.; et al. Core-shell motif construction: Highly graphitic nitrogen-doped porous carbon electrocatalysts using MOF-derived carbon@COF heterostructures as sacrificial templates. *Chem. Eng. J.* **2020**, *396*, 125154. [CrossRef]

99. Yang, W.; Greenaway, A.; Lin, X.; Matsuda, R.; Blake, A.J.; Wilson, C.; Lewis, W.; Hubberstey, P.; Kitagawa, S.; Champness, N.R.; et al. Exceptional thermal stability in a supramolecular organic framework: Porosity and gas storage. *J. Am. Chem. Soc.* **2010**, *132*, 14457–14469. [CrossRef]

100. Yin, Q.; Li, Y.-L.; Li, L.; Lü, J.; Liu, T.-F.; Cao, R. Novel Hierarchical Meso-Microporous Hydrogen-Bonded Organic Framework for Selective Separation of Acetylene and Ethylene versus Methane. *ACS Appl. Mater. Interfaces* **2019**, *11*, 17823–17827. [CrossRef]

101. Wang, B.; Lv, X.-L.; Lv, J.; Ma, L.; Lin, R.-B.; Cui, H.; Zhang, J.; Zhang, Z.; Xiang, S.; Chen, B. A novel mesoporous hydrogen-bonded organic framework with high porosity and stability. *Chem. Commun.* **2019**, *56*, 66–69. [CrossRef] [PubMed]

102. Goswami, S.; Ma, K.; Duan, J.; Kirlikovali, K.O.; Bai, J.; Hupp, J.T.; Li, P.; Farha, O.K. Understanding Diffusional Charge Transport within a Pyrene-Based Hydrogen-Bonded Organic Framework. *Langmuir* **2022**, *38*, 1533–1539. [CrossRef] [PubMed]

103. Zhou, D.-D.; Xu, Y.-T.; Lin, R.-B.; Mo, Z.-W.; Zhang, W.-X.; Zhang, J.-P. High-symmetry hydrogen-bonded organic frameworks: Air separation and crystal-to-crystal structural transformation. *Chem. Commun.* **2016**, *52*, 4991–4994. [CrossRef]

104. Nandi, S.; Chakraborty, D.; Vaidhyanathan, R. A permanently porous single molecule H-bonded organic framework for selective CO$_2$ capture. *Chem. Commun.* **2016**, *52*, 7249–7252. [CrossRef] [PubMed]

105. Wang, H.; Wu, H.; Kan, J.; Chang, G.; Yao, Z.; Li, B.; Zhou, W.; Xiang, S.; Cong-Gui Zhao, J.; Chen, B. A microporous hydrogen-bonded organic framework with amine sites for selective recognition of small molecules. *J. Mater. Chem. A* **2017**, *5*, 8292–8296. [CrossRef]

106. Ji, Q.; Takahashi, K.; Noro, S.-I.; Ishigaki, Y.; Kokado, K.; Nakamura, T.; Hisaki, I. A Hydrogen-Bonded Organic Framework Based on Pyrazinopyrazine. *Cryst. Growth Des.* **2021**, *21*, 4656–4664. [CrossRef]

107. Yin, Q.; Lü, J.; Li, H.-F.; Liu, T.-F.; Cao, R. Robust Microporous Porphyrin-Based Hydrogen-Bonded Organic Framework for Highly Selective Separation of C 2 Hydrocarbons versus Methane. *Cryst. Growth Des.* **2019**, *19*, 4157–4161. [CrossRef]

108. Zhang, X.; Li, L.; Wang, J.-X.; Wen, H.-M.; Krishna, R.; Wu, H.; Zhou, W.; Chen, Z.-N.; Li, B.; Qian, G.; et al. Selective Ethane/Ethylene Separation in a Robust Microporous Hydrogen-Bonded Organic Framework. *J. Am. Chem. Soc.* **2020**, *142*, 633–640. [CrossRef]

109. Yang, W.; Yang, F.; Hu, T.-L.; King, S.C.; Wang, H.; Wu, H.; Zhou, W.; Li, J.-R.; Arman, H.D.; Chen, B. Microporous Diaminotriazine-Decorated Porphyrin-Based Hydrogen-Bonded Organic Framework: Permanent Porosity and Proton Conduction. *Cryst. Growth Des.* **2016**, *16*, 5831–5835. [CrossRef]

110. Yang, W.; Li, B.; Wang, H.; Alduhaish, O.; Alfooty, K.; Zayed, M.A.; Li, P.; Arman, H.D.; Chen, B. A Microporous Porphyrin-Based Hydrogen-Bonded Organic Framework for Gas Separation. *Cryst. Growth Des.* **2015**, *15*, 2000–2004. [CrossRef]

111. Yang, Y.; Li, L.; Lin, R.-B.; Ye, Y.; Yao, Z.; Yang, L.; Xiang, F.; Chen, S.; Zhang, Z.; Xiang, S.; et al. Ethylene/ethane separation in a stable hydrogen-bonded organic framework through a gating mechanism. *Nat. Chem.* **2021**, *13*, 933–939. [CrossRef] [PubMed]

112. Lee, W.-G.; Yoon, T.-U.; Bae, Y.-S.; Kim, K.S.; Baek, S.B. Selective separation of Xe/Kr and adsorption of water in a microporous hydrogen-bonded organic framework. *RSC Adv.* **2019**, *9*, 36808–36814. [CrossRef] [PubMed]

113. Yang, W.; Zhou, W.; Chen, B. A Flexible Microporous Hydrogen-Bonded Organic Framework. *Cryst. Growth Des.* **2019**, *19*, 5184–5188. [CrossRef]

114. Zhang, X.; Wang, J.-X.; Li, L.; Pei, J.; Krishna, R.; Wu, H.; Zhou, W.; Qian, G.; Chen, B.; Li, B. A Rod-Packing Hydrogen-Bonded Organic Framework with Suitable Pore Confinement for Benchmark Ethane/Ethylene Separation. *Angew. Chem. Int. Ed. Engl.* **2021**, *60*, 10304–10310. [CrossRef]

115. Gong, L.; Ye, Y.; Liu, Y.; Li, Y.; Bao, Z.; Xiang, S.; Zhang, Z.; Chen, B. A Microporous Hydrogen-Bonded Organic Framework for Efficient Xe/Kr Separation. *ACS Appl. Mater. Interfaces* **2022**, *14*, 19623–19628. [CrossRef] [PubMed]

116. Wang, J.-X.; Gu, X.-W.; Lin, Y.-X.; Li, B.; Qian, G. A Novel Hydrogen-Bonded Organic Framework with Highly Permanent Porosity for Boosting Ethane/Ethylene Separation. *ACS Mater. Lett.* **2021**, *3*, 497–503. [CrossRef]

117. Li, P.; He, Y.; Arman, H.D.; Krishna, R.; Wang, H.; Weng, L.; Chen, B. A microporous six-fold interpenetrated hydrogen-bonded organic framework for highly selective separation of C$_2$H$_4$/C$_2$H$_6$. *Chem. Commun.* **2014**, *50*, 13081–13084. [CrossRef]

118. Tang, Y.; Zhang, C.; Fan, L.; Shang, Y.; Feng, Y.; Pang, J.; Cui, X.; Kong, G.; Wang, R.; Kang, Z.; et al. Regulating the Orientation of Hydrogen-Bonded Organic Framework Membranes Based on Substrate Modification. *Cryst. Growth Des.* **2021**, *21*, 5292–5299. [CrossRef]

119. Xing, G.; Bassanetti, I.; Bracco, S.; Negroni, M.; Bezuidenhout, C.; Ben, T.; Sozzani, P.; Comotti, A. A double helix of opposite charges to form channels with unique CO$_2$ selectivity and dynamics. *Chem. Sci.* **2019**, *10*, 730–736. [CrossRef]

120. Wen, H.-M.; Li, B.; Li, L.; Lin, R.-B.; Zhou, W.; Qian, G.; Chen, B. A Metal-Organic Framework with Optimized Porosity and Functional Sites for High Gravimetric and Volumetric Methane Storage Working Capacities. *Adv. Mater.* **2018**, *30*, e1704792. [CrossRef]

121. He, H.; Sun, F.; Aguila, B.; Perman, J.A.; Ma, S.; Zhu, G. A bifunctional metal–organic framework featuring the combination of open metal sites and Lewis basic sites for selective gas adsorption and heterogeneous cascade catalysis. *J. Mater. Chem. A* **2016**, *4*, 15240–15246. [CrossRef]

122. Xiong, S.; Gong, Y.; Wang, H.; Wang, H.; Liu, Q.; Gu, M.; Wang, X.; Chen, B.; Wang, Z. A new tetrazolate zeolite-like framework for highly selective CO$_2$/CH$_4$ and CO$_2$/N$_2$ separation. *Chem. Commun.* **2014**, *50*, 12101–12104. [CrossRef]

123. Nugent, P.; Belmabkhout, Y.; Burd, S.D.; Cairns, A.J.; Luebke, R.; Forrest, K.; Pham, T.; Ma, S.; Space, B.; Wojtas, L.; et al. Porous materials with optimal adsorption thermodynamics and kinetics for CO$_2$ separation. *Nature* **2013**, *495*, 80–84. [CrossRef] [PubMed]

124. Zhou, Y.; Zhang, J.; Wang, L.; Cui, X.; Liu, X.; Wong, S.S.; An, H.; Yan, N.; Xie, J.; Yu, C.; et al. Self-assembled iron-containing mordenite monolith for carbon dioxide sieving. *Science* **2021**, *373*, 315–320. [CrossRef] [PubMed]

125. Chen, L.-H.; Sun, M.-H.; Wang, Z.; Yang, W.; Xie, Z.; Su, B.-L. Hierarchically Structured Zeolites: From Design to Application. *Chem. Rev.* **2020**, *120*, 11194–11294. [CrossRef]

126. Farmahini, A.H.; Krishnamurthy, S.; Friedrich, D.; Brandani, S.; Sarkisov, L. Performance-Based Screening of Porous Materials for Carbon Capture. *Chem. Rev.* **2021**, *121*, 10666–10741. [CrossRef]

127. Wang, Z.; Zhang, S.; Chen, Y.; Zhang, Z.; Ma, S. Covalent organic frameworks for separation applications. *Chem. Soc. Rev.* **2020**, *49*, 708–735. [CrossRef] [PubMed]

128. Wen, H.-M.; Li, B.; Wang, H.; Wu, C.; Alfooty, K.; Krishna, R.; Chen, B. A microporous metal-organic framework with rare lvt topology for highly selective C$_2$H$_2$/C$_2$H$_4$ separation at room temperature. *Chem. Commun.* **2015**, *51*, 5610–5613. [CrossRef]

129. Lin, R.-B.; Li, L.; Wu, H.; Arman, H.; Li, B.; Lin, R.-G.; Zhou, W.; Chen, B. Optimized Separation of Acetylene from Carbon Dioxide and Ethylene in a Microporous Material. *J. Am. Chem. Soc.* **2017**, *139*, 8022–8028. [CrossRef]

130. Qazvini, O.T.; Babarao, R.; Shi, Z.-L.; Zhang, Y.-B.; Telfer, S.G. A Robust Ethane-Trapping Metal-Organic Framework with a High Capacity for Ethylene Purification. *J. Am. Chem. Soc.* **2019**, *141*, 5014–5020. [CrossRef]

131. Xiang, S.-C.; Zhang, Z.; Zhao, C.-G.; Hong, K.; Zhao, X.; Ding, D.-R.; Xie, M.-H.; Wu, C.-D.; Das, M.C.; Gill, R.; et al. Rationally tuned micropores within enantiopure metal-organic frameworks for highly selective separation of acetylene and ethylene. *Nat. Commun.* **2011**, *2*, 204. [CrossRef] [PubMed]

132. Chen, Y.; Qiao, Z.; Wu, H.; Lv, D.; Shi, R.; Xia, Q.; Zhou, J.; Li, Z. An ethane-trapping MOF PCN-250 for highly selective adsorption of ethane over ethylene. *Chem. Eng. Sci.* **2018**, *175*, 110–117. [CrossRef]

133. Liang, W.; Xu, F.; Zhou, X.; Xiao, J.; Xia, Q.; Li, Y.; Li, Z. Ethane selective adsorbent Ni(bdc)(ted)0.5 with high uptake and its significance in adsorption separation of ethane and ethylene. *Chem. Eng. Sci.* **2016**, *148*, 275–281. [CrossRef]

134. Liao, P.-Q.; Zhang, W.-X.; Zhang, J.-P.; Chen, X.-M. Efficient purification of ethene by an ethane-trapping metal-organic framework. *Nat. Commun.* **2015**, *6*, 8697. [CrossRef]

135. Li, L.; Lin, R.-B.; Krishna, R.; Li, H.; Xiang, S.; Wu, H.; Li, J.; Zhou, W.; Chen, B. Ethane/ethylene separation in a metal-organic framework with iron-peroxo sites. *Science* **2018**, *362*, 443–446. [CrossRef]

136. Chen, Y.; Wu, H.; Lv, D.; Shi, R.; Chen, Y.; Xia, Q.; Li, Z. Highly Adsorptive Separation of Ethane/Ethylene by An Ethane-Selective MOF MIL-142A. *Ind. Eng. Chem. Res.* **2018**, *57*, 4063–4069. [CrossRef]

137. Lv, D.; Shi, R.; Chen, Y.; Wu, Y.; Wu, H.; Xi, H.; Xia, Q.; Li, Z. Selective Adsorption of Ethane over Ethylene in PCN-245: Impacts of Interpenetrated Adsorbent. *ACS Appl. Mater. Interfaces* **2018**, *10*, 8366–8373. [CrossRef]

138. Lin, R.-B.; Wu, H.; Li, L.; Tang, X.-L.; Li, Z.; Gao, J.; Cui, H.; Zhou, W.; Chen, B. Boosting Ethane/Ethylene Separation within Isoreticular Ultramicroporous Metal-Organic Frameworks. *J. Am. Chem. Soc.* **2018**, *140*, 12940–12946. [CrossRef]

139. Böhme, U.; Barth, B.; Paula, C.; Kuhnt, A.; Schwieger, W.; Mundstock, A.; Caro, J.; Hartmann, M. Ethene/ethane and propene/propane separation via the olefin and paraffin selective metal-organic framework adsorbents CPO-27 and ZIF-8. *Langmuir* **2013**, *29*, 8592–8600. [CrossRef] [PubMed]

140. Gücüyener, C.; van den Bergh, J.; Gascon, J.; Kapteijn, F. Ethane/ethene separation turned on its head: Selective ethane adsorption on the metal-organic framework ZIF-7 through a gate-opening mechanism. *J. Am. Chem. Soc.* **2010**, *132*, 17704–17706. [CrossRef]

141. Wang, L.; Yang, L.; Gong, L.; Krishna, R.; Gao, Z.; Tao, Y.; Yin, W.; Xu, Z.; Luo, F. Constructing redox-active microporous hydrogen-bonded organic framework by imide-functionalization: Photochromism, electrochromism, and selective adsorption of C2H2 over CO$_2$. *Chem. Eng. J.* **2020**, *383*, 123117. [CrossRef]

142. Cha, J.; Jo, Y.S.; Jeong, H.; Han, J.; Nam, S.W.; Song, K.H.; Yoon, C.W. Ammonia as an efficient COX-free hydrogen carrier: Fundamentals and feasibility analyses for fuel cell applications. *Appl. Energy* **2018**, *224*, 194–204. [CrossRef]

143. Rieth, A.J.; Dincă, M. Controlled Gas Uptake in Metal-Organic Frameworks with Record Ammonia Sorption. *J. Am. Chem. Soc.* **2018**, *140*, 3461–3466. [CrossRef] [PubMed]

144. van Humbeck, J.F.; McDonald, T.M.; Jing, X.; Wiers, B.M.; Zhu, G.; Long, J.R. Ammonia capture in porous organic polymers densely functionalized with Brønsted acid groups. *J. Am. Chem. Soc.* **2014**, *136*, 2432–2440. [CrossRef] [PubMed]

145. Doonan, C.J.; Tranchemontagne, D.J.; Glover, T.G.; Hunt, J.R.; Yaghi, O.M. Exceptional ammonia uptake by a covalent organic framework. *Nat. Chem.* **2010**, *2*, 235–238. [CrossRef] [PubMed]

146. Kang, D.W.; Kang, M.; Moon, M.; Kim, H.; Eom, S.; Choe, J.H.; Lee, W.R.; Hong, C.S. PDMS-coated hypercrosslinked porous organic polymers modified via double postsynthetic acidifications for ammonia capture. *Chem. Sci.* **2018**, *9*, 6871–6877. [CrossRef]

147. Barin, G.; Peterson, G.W.; Crocellà, V.; Xu, J.; Colwell, K.A.; Nandy, A.; Reimer, J.A.; Bordiga, S.; Long, J.R. Highly effective ammonia removal in a series of Brønsted acidic porous polymers: Investigation of chemical and structural variations. *Chem. Sci.* **2017**, *8*, 4399–4409. [CrossRef] [PubMed]

148. Rieth, A.J.; Tulchinsky, Y.; Dincă, M. High and Reversible Ammonia Uptake in Mesoporous Azolate Metal-Organic Frameworks with Open Mn, Co, and Ni Sites. *J. Am. Chem. Soc.* **2016**, *138*, 9401–9404. [CrossRef]

149. Chen, L.; Reiss, P.S.; Chong, S.Y.; Holden, D.; Jelfs, K.E.; Hasell, T.; Little, M.A.; Kewley, A.; Briggs, M.E.; Stephenson, A.; et al. Separation of rare gases and chiral molecules by selective binding in porous organic cages. *Nat. Mater.* **2014**, *13*, 954–960. [CrossRef]

150. Chakraborty, D.; Nandi, S.; Sinnwell, M.A.; Liu, J.; Kushwaha, R.; Thallapally, P.K.; Vaidhyanathan, R. Hyper-Cross-linked Porous Organic Frameworks with Ultramicropores for Selective Xenon Capture. *ACS Appl. Mater. Interfaces* **2019**, *11*, 13279–13284. [CrossRef]

151. Lawler, K.V.; Hulvey, Z.; Forster, P.M. Nanoporous metal formates for krypton/xenon separation. *Chem. Commun.* **2013**, *49*, 10959–10961. [CrossRef]

152. Wang, H.; Yao, K.; Zhang, Z.; Jagiello, J.; Gong, Q.; Han, Y.; Li, J. The first example of commensurate adsorption of atomic gas in a MOF and effective separation of xenon from other noble gases. *Chem. Sci.* **2014**, *5*, 620–624. [CrossRef]

153. Meek, S.T.; Teich-McGoldrick, S.L.; Perry, J.J.; Greathouse, J.A.; Allendorf, M.D. Effects of Polarizability on the Adsorption of Noble Gases at Low Pressures in Monohalogenated Isoreticular Metal–Organic Frameworks. *J. Phys. Chem. C* **2012**, *116*, 19765–19772. [CrossRef]

154. Mohamed, M.H.; Elsaidi, S.K.; Pham, T.; Forrest, K.A.; Schaef, H.T.; Hogan, A.; Wojtas, L.; Xu, W.; Space, B.; Zaworotko, M.J.; et al. Hybrid Ultra-Microporous Materials for Selective Xenon Adsorption and Separation. *Angew. Chem. Int. Ed. Engl.* **2016**, *55*, 8285–8289. [CrossRef] [PubMed]

155. Saptiama, I.; Kaneti, Y.V.; Oveisi, H.; Suzuki, Y.; Tsuchiya, K.; Takai, K.; Sakae, T.; Pradhan, S.; Hossain, M.S.A.; Fukumitsu, N.; et al. Molybdenum Adsorption Properties of Alumina-Embedded Mesoporous Silica for Medical Radioisotope Production. *BCSJ* **2018**, *91*, 195–200. [CrossRef]

156. Kaushik, A.; Marvaniya, K.; Kulkarni, Y.; Bhatt, D.; Bhatt, J.; Mane, M.; Suresh, E.; Tothadi, S.; Patel, K.; Kushwaha, S. Large-area self-standing thin film of porous hydrogen-bonded organic framework for efficient uranium extraction from seawater. *Chem* **2022**, *8*, 2749–2765. [CrossRef]

157. Liu, R.; Zhang, W.; Chen, Y.; Wang, Y. Uranium (VI) adsorption by copper and copper/iron bimetallic central MOFs. *Colloids Surf. A Physicochem. Eng. Asp.* **2020**, *587*, 124334. [CrossRef]

158. Zhang, G.; Fang, Y.; Wang, Y.; Liu, L.; Mei, D.; Ma, F.; Meng, Y.; Dong, H.; Zhang, C. Synthesis of amino acid modified MIL-101 and efficient uranium adsorption from water. *J. Mol. Liq.* **2022**, *349*, 118095. [CrossRef]

159. Liu, J.-M.; Yin, X.-H.; Liu, T. Amidoxime-functionalized metal-organic frameworks UiO-66 for U(VI) adsorption from aqueous solution. *J. Taiwan Inst. Chem. Eng.* **2019**, *95*, 416–423. [CrossRef]

160. Su, S.; Che, R.; Liu, Q.; Liu, J.; Zhang, H.; Li, R.; Jing, X.; Wang, J. Zeolitic Imidazolate Framework-67: A promising candidate for recovery of uranium (VI) from seawater. *Colloids Surf. A Physicochem. Eng. Asp.* **2018**, *547*, 73–80. [CrossRef]

161. Mei, D.; Li, H.; Liu, L.; Jiang, L.; Zhang, C.; Wu, X.; Dong, H.; Ma, F. Efficient uranium adsorbent with antimicrobial function: Oxime functionalized ZIF-90. *Chem. Eng. J.* **2021**, *425*, 130468. [CrossRef]

162. Li, F.-F.; Cui, W.-R.; Jiang, W.; Zhang, C.-R.; Liang, R.-P.; Qiu, J.-D. Stable sp2 carbon-conjugated covalent organic framework for detection and efficient adsorption of uranium from radioactive wastewater. *J. Hazard. Mater.* **2020**, *392*, 122333. [CrossRef] [PubMed]

163. Li, Z.D.; Zhang, H.Q.; Xiong, X.H.; Luo, F. U(VI) adsorption onto covalent organic frameworks-TpPa-1. *J. Solid State Chem.* **2019**, *277*, 484–492. [CrossRef]

164. Zhang, J.; Zhou, L.; Jia, Z.; Li, X.; Qi, Y.; Yang, C.; Guo, X.; Chen, S.; Long, H.; Ma, L. Construction of covalent organic framework with unique double-ring pore for size-matching adsorption of uranium. *Nanoscale* **2020**, *12*, 24044–24053. [CrossRef] [PubMed]

165. Li, X.; Qi, Y.; Yue, G.; Wu, Q.; Li, Y.; Zhang, M.; Guo, X.; Li, X.; Ma, L.; Li, S. Solvent- and catalyst-free synthesis of an azine-linked covalent organic framework and the induced tautomerization in the adsorption of U(vi) and Hg(ii). *Green Chem.* **2019**, *21*, 649–657. [CrossRef]

166. Qin, X.; Tang, X.; Ma, Y.; Xu, H.; Xu, Q.; Yang, W.; Gu, C. Decorating Covalent Organic Frameworks with High-density Chelate Groups for Uranium Extraction. *Chem. Res. Chin. Univ.* **2022**, *38*, 433–439. [CrossRef]

167. Li, S.; Bai, H.; Wang, J.; Jing, X.; Liu, Q.; Zhang, M.; Chen, R.; Liu, L.; Jiao, C. In situ grown of nano-hydroxyapatite on magnetic CaAl-layered double hydroxides and its application in uranium removal. *Chem. Eng. J.* **2012**, *193*, 372–380. [CrossRef]

168. Fan, F.-L.; Qin, Z.; Bai, J.; Rong, W.-D.; Fan, F.-Y.; Tian, W.; Wu, X.-L.; Wang, Y.; Zhao, L. Rapid removal of uranium from aqueous solutions using magnetic Fe3O4@SiO2 composite particles. *J. Environ. Radioact.* **2012**, *106*, 40–46. [CrossRef]

169. Sarafraz, H.; Minuchehr, A.; Alahyarizadeh, G.; Rahimi, Z. Synthesis of enhanced phosphonic functional groups mesoporous silica for uranium selective adsorption from aqueous solutions. *Sci. Rep.* **2017**, *7*, 11675. [CrossRef]

170. Ilaiyaraja, P.; Deb, A.K.S.; Sivasubramanian, K.; Ponraju, D.; Venkatraman, B. Adsorption of uranium from aqueous solution by PAMAM dendron functionalized styrene divinylbenzene. *J. Hazard. Mater.* **2013**, *250*, 155–166. [CrossRef]

171. Sureshkumar, M.K.; Das, D.; Mallia, M.B.; Gupta, P.C. Adsorption of uranium from aqueous solution using chitosan-tripolyphosphate (CTPP) beads. *J. Hazard. Mater.* **2010**, *184*, 65–72. [CrossRef] [PubMed]

172. Bai, J.; Ma, X.; Yan, H.; Zhu, J.; Wang, K.; Wang, J. A novel functional porous organic polymer for the removal of uranium from wastewater. *Microporous Mesoporous Mater.* **2020**, *306*, 110441. [CrossRef]

173. Ghasemi, M.; Keshtkar, A.R.; Dabbagh, R.; Jaber Safdari, S. Biosorption of uranium(VI) from aqueous solutions by Ca-pretreated Cystoseira indica alga: Breakthrough curves studies and modeling. *J. Hazard. Mater.* **2011**, *189*, 141–149. [CrossRef] [PubMed]

174. Zhang, J.; Chen, H.; Song, J.; Deng, H.; Chen, Z.; Lin, Z. Immobilization of Uranium at Nanoscale by Bacillus cereus 12-2 at Different U(VI) Concentration. *J. Nanosci. Nanotechnol.* **2019**, *19*, 7131–7138. [CrossRef]

175. Saini, A.S.; Melo, J.S. Biosorption of uranium by melanin: Kinetic, equilibrium and thermodynamic studies. *Bioresour. Technol.* **2013**, *149*, 155–162. [CrossRef]

176. Wagner, M.; Andrew Lin, K.-Y.; Oh, W.-D.; Lisak, G. Metal-organic frameworks for pesticidal persistent organic pollutants detection and adsorption–A mini review. *J. Hazard. Mater.* **2021**, *413*, 125325. [CrossRef]

177. Wang, W.; Deng, S.; Ren, L.; Li, D.; Wang, W.; Vakili, M.; Wang, B.; Huang, J.; Wang, Y.; Yu, G. Stable Covalent Organic Frameworks as Efficient Adsorbents for High and Selective Removal of an Aryl-Organophosphorus Flame Retardant from Water. *ACS Appl. Mater. Interfaces* **2018**, *10*, 30265–30272. [CrossRef]

178. Choong, Z.-Y.; Lin, K.-Y.A.; Oh, W.-D. Copper ferrite anchored on hexagonal boron nitride as peroxymonosulfate activator for ciprofloxacin removal. *Mater. Lett.* **2021**, *285*, 129079. [CrossRef]

179. Lv, Y.; Qin, X.; Hu, K.; Ye, F.; Zhao, S. Microporous hydrogen-bond organic frameworks-based SALDI-TOF MS for simultaneous enrichment and high sensitivity detection of paraquat and chlormequat. *Sens. Actuators B Chem.* **2022**, *353*, 131132. [CrossRef]

180. Ghosh, M.K.; Giri, S.; Ghorai, T.K. Single pot reaction of Co(III) and Ni(II) hydrogen-bonded organic frameworks and multidisciplinary application in dye adsorption, separation and DNA binding. *J. Mol. Struct.* **2020**, *1206*, 127727. [CrossRef]

181. Yang, J.; Wang, J.; Zhang, X.; Chen, M.; Tian, B.; Wang, N.; Huang, X.; Hao, H. Exploration of hydrogen-bonded organic framework (HOF) as highly efficient adsorbent for rhodamine B and methyl orange. *Microporous Mesoporous Mater.* **2022**, *330*, 111624. [CrossRef]

182. Jedynak, K.; Wideł, D.; Rędzia, N. Removal of Rhodamine B (A Basic Dye) and Acid Yellow 17 (An Acidic Dye) from Aqueous Solutions by Ordered Mesoporous Carbon and Commercial Activated Carbon. *Colloids Interfaces* **2019**, *3*, 30. [CrossRef]

183. Yönten, V.; Sanyürek, N.K.; Kivanç, M.R. A thermodynamic and kinetic approach to adsorption of methyl orange from aqueous solution using a low cost activated carbon prepared from *Vitis vinifera* L. *Surf. Interfaces* **2020**, *20*, 100529. [CrossRef]

184. Duan, S.; Li, J.; Liu, X.; Wang, Y.; Zeng, S.; Shao, D.; Hayat, T. HF-Free Synthesis of Nanoscale Metal–Organic Framework NMIL-100(Fe) as an Efficient Dye Adsorbent. *ACS Sustain. Chem. Eng.* **2016**, *4*, 3368–3378. [CrossRef]

185. Xu, T.; Hou, X.; Liu, S.; Liu, B. One-step synthesis of magnetic and porous Ni@MOF-74(Ni) composite. *Microporous Mesoporous Mater.* **2018**, *259*, 178–183. [CrossRef]

186. Lv, S.-W.; Liu, J.-M.; Ma, H.; Wang, Z.-H.; Li, C.-Y.; Zhao, N.; Wang, S. Simultaneous adsorption of methyl orange and methylene blue from aqueous solution using amino functionalized Zr-based MOFs. *Microporous Mesoporous Mater.* **2019**, *282*, 179–187. [CrossRef]

187. Li, Y.; Zhou, K.; He, M.; Yao, J. Synthesis of ZIF-8 and ZIF-67 using mixed-base and their dye adsorption. *Microporous Mesoporous Mater.* **2016**, *234*, 287–292. [CrossRef]

188. Wu, S.-C.; Yu, L.-L.; Xiao, F.-F.; You, X.; Yang, C.; Cheng, J.-H. Synthesis of aluminum-based MOF/graphite oxide composite and enhanced removal of methyl orange. *J. Alloy. Compd.* **2017**, *724*, 625–632. [CrossRef]

189. Liang, X.; Ni, Z.; Zhao, L.; Ge, B.; Zhao, H.; Li, W. Improving surface areas of covalent organic framework with surfactant assisted solvothermal method and its adsorption properties for rhodamine B. *Mater. Chem. Phys.* **2021**, *270*, 124725. [CrossRef]

190. Garai, B.; Shetty, D.; Skorjanc, T.; Gándara, F.; Naleem, N.; Varghese, S.; Sharma, S.K.; Baias, M.; Jagannathan, R.; Olson, M.A.; et al. Taming the Topology of Calix4arene-Based 2D-Covalent Organic Frameworks: Interpenetrated vs Noninterpenetrated Frameworks and Their Selective Removal of Cationic Dyes. *J. Am. Chem. Soc.* **2021**, *143*, 3407–3415. [CrossRef]

191. Hou, Y.; Zhang, X.; Wang, C.; Qi, D.; Gu, Y.; Wang, Z.; Jiang, J. Novel imine-linked porphyrin covalent organic frameworks with good adsorption removing properties of RhB. *New J. Chem.* **2017**, *41*, 6145–6151. [CrossRef]

192. Xu, S.-X.; Yao, Z.-Q.; Zhang, Y.-H. A covalent organic framework exhibiting amphiphilic selective adsorption toward ionic organic dyes tuned by pH value. *Eur. Polym. J.* **2020**, *133*, 109764. [CrossRef]

193. Suner, S.S.; Demirci, S.; Sutekin, D.S.; Yilmaz, S.; Sahiner, N. Thiourea-Isocyanate-Based Covalent Organic Frameworks with Tunable Surface Charge and Surface Area for Methylene Blue and Methyl Orange Removal from Aqueous Media. *Micromachines* **2022**, *13*, 938. [CrossRef]

194. Gao, X.; Lu, W.; Wang, Y.; Song, X.; Wang, C.; Kirlikovali, K.O.; Li, P. Recent advancements of photo- and electro-active hydrogen-bonded organic frameworks. *Sci. China Chem.* **2022**, *65*, 2077–2095. [CrossRef]

195. Li, T.; Liu, B.-T.; Fang, Z.-B.; Yin, Q.; Wang, R.; Liu, T.-F. Integrating active C3N4 moieties in hydrogen-bonded organic frameworks for efficient photocatalysis. *J. Mater. Chem. A* **2021**, *9*, 4687–4691. [CrossRef]

196. Aitchison, C.M.; Kane, C.M.; McMahon, D.P.; Spackman, P.R.; Pulido, A.; Wang, X.; Wilbraham, L.; Chen, L.; Clowes, R.; Zwijnenburg, M.A.; et al. Photocatalytic proton reduction by a computationally identified, molecular hydrogen-bonded framework. *J. Mater. Chem. A* **2020**, *8*, 7158–7170. [CrossRef]

197. Yu, B.; Li, L.; Liu, S.; Wang, H.; Liu, H.; Lin, C.; Liu, C.; Wu, H.; Zhou, W.; Li, X.; et al. Robust Biological Hydrogen-Bonded Organic Framework with Post-Functionalized Rhenium(I) Sites for Efficient Heterogeneous Visible-Light-Driven CO$_2$ Reduction. *Angew. Chem. Int. Ed. Engl.* **2021**, *60*, 8983–8989. [CrossRef] [PubMed]

198. Bai, Y.; Wilbraham, L.; Slater, B.J.; Zwijnenburg, M.A.; Sprick, R.S.; Cooper, A.I. Accelerated Discovery of Organic Polymer Photocatalysts for Hydrogen Evolution from Water through the Integration of Experiment and Theory. *J. Am. Chem. Soc.* **2019**, *141*, 9063–9071. [CrossRef]

199. Bi, S.; Lan, Z.-A.; Paasch, S.; Zhang, W.; He, Y.; Zhang, C.; Liu, F.; Wu, D.; Zhuang, X.; Brunner, E.; et al. Substantial Cyano-Substituted Fully sp^2-Carbon-Linked Framework: Metal-Free Approach and Visible-Light-Driven Hydrogen Evolution. *Adv. Funct. Mater.* **2017**, *27*, 1703146. [CrossRef]

200. He, X.-T.; Luo, Y.-H.; Zheng, Z.-Y.; Wang, C.; Wang, J.-Y.; Hong, D.-L.; Zhai, L.-H.; Guo, L.-H.; Sun, B.-W. Porphyrin-Based Hydrogen-Bonded Organic Frameworks for the Photocatalytic Degradation of 9,10-Diphenylanthracene. *ACS Appl. Nano Mater.* **2019**, *2*, 7719–7727. [CrossRef]

201. Wang, J.; Mao, Y.; Zhang, R.; Zeng, Y.; Li, C.; Zhang, B.; Zhu, J.; Ji, J.; Liu, D.; Gao, R.; et al. In Situ Assembly of Hydrogen-Bonded Organic Framework on Metal-Organic Framework: An Effective Strategy for Constructing Core-Shell Hybrid Photocatalyst. *Adv. Sci. (Weinh.)* **2022**, *9*, e2204036. [CrossRef]

202. Li, Y.-L.; Wang, H.-L.; Chen, Z.-C.; Zhu, Z.-H.; Liu, Y.-C.; Yang, R.-Y.; Liang, F.-P.; Zou, H.-H. Lanthanoid hydrogen-bonded organic frameworks: Enhancement of luminescence by the coordination-promoted antenna effect and applications in heavy-metal ion sensing and sterilization. *Chem. Eng. J.* **2023**, *451*, 138880. [CrossRef]

203. Fan, Z.; Zheng, S.; Zhang, H.; Chen, K.; Li, Y.; Liu, C.; Xiang, S.; Zhang, Z. Amidinium sulfonate hydrogen-bonded organic framework with fluorescence amplification function for sensitive aniline detection. *Chin. Chem. Lett.* **2022**, *33*, 4317–4320. [CrossRef]

204. Lin, Z.-J.; Qin, J.-Y.; Zhan, X.-P.; Wu, K.; Cao, G.-J.; Chen, B. Robust Mesoporous Functional Hydrogen-Bonded Organic Framework for Hypochlorite Detection. *ACS Appl. Mater. Interfaces* **2022**, *14*, 21098–21105. [CrossRef] [PubMed]

205. Zhu, K.; Xu, X.; Yan, B. Eu(iii)-Functionalized HOFs based on machine learning-assisted fluorescence sensing: Discrimination of quinolones via PCA and BPNN models. *J. Mater. Chem. C* **2022**, *10*, 10320–10329. [CrossRef]

206. Guo, G.; Wang, D.; Zheng, X.; Bi, X.; Liu, S.; Sun, L.; Zhao, Y. Construction of tetraphenylethylene-based fluorescent hydrogen-bonded organic frameworks for detection of explosives. *Dye. Pigment.* **2022**, *197*, 109881. [CrossRef]

207. Wang, B.; He, R.; Xie, L.-H.; Lin, Z.-J.; Zhang, X.; Wang, J.; Huang, H.; Zhang, Z.; Schanze, K.S.; Zhang, J.; et al. Microporous Hydrogen-Bonded Organic Framework for Highly Efficient Turn-Up Fluorescent Sensing of Aniline. *J. Am. Chem. Soc.* **2020**, *142*, 12478–12485. [CrossRef]